Two hundred thirty years of relative sea level changes due to climate and megathrust tectonics recorded in coral microatolls of Martinique (French West Indies)

Jennifer Weil-Accardo, Nathalie Feuillet, Eric Jacques, Pierre Deschamps, François Beauducel, Paul Tapponnier, Guy Cabioch, Jean-Marie Saurel, John Galetzka

AGU PUBLICATIONS

JGR

Journal of Geophysical Research: Solid Earth

RESEARCH ARTICLE
10.1002/2015JB012406

Key Points:
- Relative sea level changes in Martinique since approximately two centuries
- Relative sea level changes associated with past earthquakes (1839 and 1946 M7+ earthquakes)
- Discussion about the coupling of the Lesser Antilles megathrust with coral microatolls

Supporting Information:
- Supporting Information S1

Correspondence to:
J. Weil-Accardo,
weilaccardo@ipgp.fr

Citation:
Weil-Accardo, J., N. Feuillet, E. Jacques, P. Deschamps, F. Beauducel, G. Cabioch, P. Tapponnier, J.-M. Saurel, and J. Galetzka (2016), Two hundred thirty years of relative sea level changes due to climate and megathrust tectonics recorded in coral microatolls of Martinique (French West Indies), *J. Geophys. Res. Solid Earth*, *121*, 2873–2903, doi:10.1002/2015JB012406.

Received 3 AUG 2015
Accepted 24 FEB 2016
Accepted article online 27 FEB 2016
Published online 8 APR 2016

Two hundred thirty years of relative sea level changes due to climate and megathrust tectonics recorded in coral microatolls of Martinique (French West Indies)

Jennifer Weil-Accardo[1], Nathalie Feuillet[1], Eric Jacques[1], Pierre Deschamps[2], François Beauducel[1], Guy Cabioch[3], Paul Tapponnier[4], Jean-Marie Saurel[1], and John Galetzka[5]

[1]Institut de Physique du Globe de Paris, UMR 7154, CNRS Sorbonne Paris Cité, Paris, France, [2]CEREGE, UM34 Aix-Marseille Université-CNRS-IRD, Aix-en-Provence, France, [3]IRD, Bondy, France, [4]Earth Observatory of Singapore, Nanyang Technological University, Singapore, [5]Tectonics Observatory, California Institute of Technology, Pasadena, California, USA

Abstract We sampled six coral microatolls that recorded the relative sea level changes over the last 230 years east of Martinique, on fringing reefs in protected bays. The microatolls are cup-shaped, which is characteristic of corals that have been experiencing submergence. X-ray analysis of coral slices and reconstructions of the highest level of survival (HLS) curves show that they have submerged at rates of a few millimeters per year. Their morphology reveals changes in submergence rate around 1829 ± 11, 1895, and 1950. Tide gauges available in the region indicate a regional sea level rise at a constant mean rate of 1.1 ± 0.8 mm/yr, which contrasts with our coral record, implying additional tectonic subsidence. Comparing our coral morphology with that of synthetic corals generated with Matlab by using the Key West tide gauge record (Florida), we show that their growth was controlled by tectonics and that a sudden relative sea level increase drowned them around 1950. Simple elastic models show that this sudden submergence probably occurred during the 21 May 1946 earthquake, which ruptured the plate interface in front of Martinique, in the mantle wedge, in an area of sustained seismic activity. The 1839 *M*8+ earthquake probably occurred in the same area. Long-term subsidence of microatolls indicates that this deep portion of the megathrust is probably locked down to 60 km depth during the interseismic period. Our oldest coral recorded a long-lasting period (50 years) of stable relative sea level after the 1839 earthquake, indicating that transient interseismic strain rate variations may occur in the Lesser Antilles.

1. Introduction

The numerous islands of the Lesser Antilles (Figure 1a) are densely populated and touristic zones with extensive infrastructure and numerous towns along the coasts. They are especially vulnerable to global sea level rise and also exposed to multiple threats (volcanic eruptions, hurricanes, earthquakes, and coastal erosion) that can generate relative sea level changes. The islands of the arc lie above a megathrust interface where the American Plates subduct under the Caribbean Plate at a rate of 2 cm/yr. It has been documented in several subduction zones that the seismic cycle along such structure is associated with vertical deformation of the overriding plate [e.g., *Chlieh et al.*, 2004]. Between large earthquakes, the so-called interseismic period is characterized by land deformation at rates of a few millimeters per year over several decades, centuries, or millennia. In coastal areas, this may induce a relative increase or decrease in sea level at a rate that can be much faster than the regional sea level rise. Megathrust earthquakes that typically occur only every several centuries or millennia may induce metric-scale sudden subsidence or uplift of coastline, observed as sudden submergence or emergence along the coast.

Within the framework of global warming, evaluation of the relative sea level changes induced by climate and tectonics in the Lesser Antilles is a pressing goal for the near future. Such measurements are relevant to both the regional variability of climate-driven sea level rise in the Caribbean and the seismic potential of the Lesser Antilles megathrust.

However, in the Lesser Antilles, the instrumental data for measuring relative sea level variations are too sparse and often very limited in duration, leading to a poor knowledge of the history of past and ongoing relative sea level changes along the arc. Taking advantage of the ubiquitous corals in this tropical area, we use massive

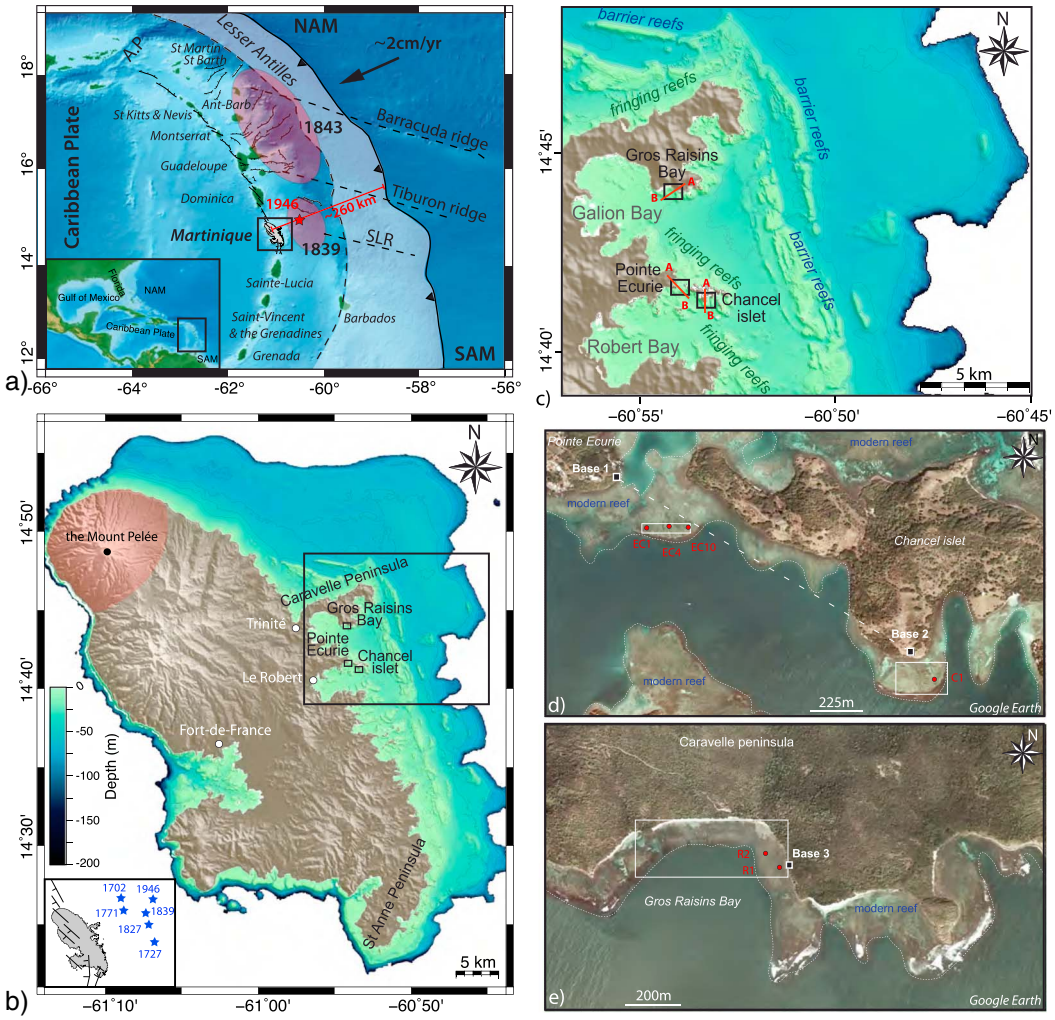

Figure 1. Reefs of Martinique. (a) Geodynamic setting. Bathymetry and topography: SRTM30+ (horizontal resolution: 900 m). Active faults from *Feuillet* [2000], *Feuillet et al.* [2002, 2004, 2011a], and *Leclerc* [2014]. Convergence rate and direction from *DeMets et al.* [2000]. A.P: Anegada Passage, SLR: Sainte-Lucia ridge. NAM and SAM: North American and South American Plates. Ant-Barb: Antigua and Barbuda islands. Red ellipses: rupture areas for 11 January 1839 *M*8 and 8 February 1843 *M*8.5 earthquakes [*Feuillet et al.*, 2011a]. Red star: epicentral location for the 21 May 1946 earthquake [*Dorel*, 1981; *Feuillard*, 1985]. Black line with triangles: accretionary prism frontal thrust. Dashed black line: main negative gravity anomaly corresponding to the Lesser Antilles backstop [*Westbrook et al.*, 1988; *Bowin*, 1976; *Laigle et al.*, 2013; *Evain et al.*, 2013]. Light colored area: accretionary prism. Black rectangle: Martinique Island. Inset: Broad context of the study (Figure 13). Black rectangle: Lesser Antilles arc. (b) Martinique reef complex. Topographic DEM: IGN data (horizontal resolution: 50 m). Topography and bathymetry between +50 m and −60 m: Litto3D LIDAR data (horizontal resolution: 5 m). Bathymetry from −60 m to −200 m: SHOM data (horizontal resolution: 50 m). One isobath is drawn every 10 m. White dots: main towns. Large black rectangle: area of Figure 1c). Small black rectangles: sampling sites in Figures 1d) and 1e). Inset: significant past earthquakes (blue stars) offshore Martinique [*Dorel*, 1981; *Feuillard*, 1985] and active faults from *Savry* [2007] and *Feuillet et al.* [2011a]. (c) Detail of Robert and Galion Bays. Topograph and bathymetry as in Figure 1b). Black rectangles: sampling sites of Pointe Ecurie, Chancel islet, and Gros Raisins Bay. Red lines: topographic and bathymetric profiles in Figure 2a and Figures S4a and S5a in the supporting information. (d and e) Google Earth screenshots of the three sampling areas. Black squares: total station bases for the sites. The total station bases of Pointe Ecurie and Chancel islet have been connected (dashed white line). White rectangles: surveyed reef in Figures 2, 3, S4, and S5. Red dots: sampled corals.

coral colonies that adopted a microatoll shape. Microatolls are known to record relative sea level changes with a precision of a few centimeters [e.g., *Taylor et al.*, 1987; *Woodroffe and McLean*, 1990; *Zachariasen et al.*, 1999, 2000]. Their use allows us to extend the sparse network of existent tide gauges in time and space and offers the opportunity of reconstructing past relative sea levels in areas where tide gauges are not installed [*Woodroffe and McLean*, 1990].

The upward growth of a coral microatoll is limited by its highest level of survival (HLS), which is typically related to the lowest tide level [*Meltzner et al.*, 2010]. As HLS fluctuations are linked to relative sea level variations [*Zachariasen et al.*, 1999, 2000], analysis of coral microatolls allows the reconstruction of relative sea level changes through time by recording the HLS changes in their stratigraphy. Since the coral microatoll adapts its growth in response to relative sea level changes [e.g., *Stoddart and Scoffin*, 1979; *Scoffin et al.*, 1978; *Taylor et al.*, 1987; *Hopley*, 2011], in the case of stable relative sea level, the coral mainly grows outward and develops a flat shape. In the case of submergence, upward growth is promoted and the coral displays a cup shape surrounded by a higher living rim. If the coral experiences a sea level drop, the emerged part of the coral dies while the deeper part continues to grow below the sea level. This leads to a microatoll with a hat shape.

Several studies of coral microatolls concentrated in the Indian and Pacific Oceans analyze sea level at interannual to millenial timescales [*Woodroffe et al.*, 1990; *Woodroffe and Gagan*, 2000; *Smithers and Woodroffe*, 2001; *Woodroffe et al.*, 2012]. Additionally, the use of fossil coral microatolls in the northern South China Sea allowed *Yu et al.* [2009] to infer a 450 year long record of sea level fluctuations in the mid-Holocene.

In Vanuatu and in Indonesia, coral microatolls have been used to document vertical deformation related to the New Hebrides and Sumatra subduction zones, respectively. Recent and paleo-megathrust earthquakes have been studied in both locations [*Taylor et al.*, 1980, 1982; *Zachariasen et al.*, 1999; *Natawidjaja et al.*, 2006; *Meltzner et al.*, 2006; *Sieh et al.*, 2008; *Meltzner et al.*, 2010, 2012; *Philibosian et al.*, 2012; *Meltzner et al.*, 2015], and the history of interseismic strain accumulation on the megathrust interface between earthquakes has been documented mainly in Indonesia [*Zachariasen et al.*, 2000; *Natawidjaja et al.*, 2007; *Meltzner et al.*, 2010, 2012; *Philibosian et al.*, 2014; *Meltzner et al.*, 2015].

We investigated the eastern part of Martinique Island, near the Caravelle peninsula (Figures 1b–1d), which is the area closest to the trench, and where corals abound. Numerous historical earthquakes have been reported offshore the Caravelle peninsula (September 1702, 7 November 1727, February 1771, 21 December 1827, 11 January 1839, and 21 May 1946, of magnitude 7, 7, 6, 7, 8, and 7, respectively, according to *Robson* [1964], *Dorel* [1981], *Feuillard* [1985], *Feuillet et al.* [2011a]) (inset in Figure 1b) and sustained seismic activity has been identified in that area by *Laigle et al.* [2013] and *Ruiz et al.* [2013].

First, we describe the methodology used. In the second part, we present the sites we studied. The third section is dedicated to the description of the stratigraphy and the morphology of six microatolls that allows us to describe the century-scale sea level variations. We then discuss the causes of the relative sea level changes recorded by microatolls, by comparing the coral record to the regional sea level rise derived from tide gauges. Toward this goal, we developed a Matlab code to simulate the growth of a microatoll in different contexts of relative sea level variations (steady relative sea level increase, sudden tectonic deformation, and rate increase of relative sea level change). We also compare the morphology of our microatolls from Martinique to that of coral we sampled farther north in Haiti in a different geodynamic context [*Weil-Accardo et al.*, 2016]. Finally, we discuss our results in terms of climate and tectonics with the help of simple and widely used elastic dislocation models that relate upper plate vertical deformation to fault motion during different stages of the seismic cycle on the megathrust.

2. Methodology

2.1. Survey and Sampling

All reefs around Martinique Island were first surveyed via helicopter flight to identify sites where coral microatolls are growing. We then explored the most promising reefs by boat and sampled coral microatolls between 28 January 2008 and 7 February 2008.

Before sampling, each site was mapped using a total station. We measured the top of the external living rim of all coral microatolls to determine the modern HLS elevation over the whole area. On average, the 2σ range of the modern HLS is about $\pm$10 cm across many corals at a given site and between $\pm$2 cm and $\pm$10 cm for a given microatoll. These values are similar to HLS variations measured in Indonesia

[*Zachariasen*, 1998; *Zachariasen et al.*, 1999, 2000; *Natawidjaja et al.*, 2004] and in Vanuatu [*Taylor et al.*, 1980, 1987]. To constrain the relationship between the HLS and the tidal range, we also measured the water level at all sites.

The total station allowed us to measure altitude and distance, relative to the total station base, with millimetric precision. Uncertainty of the survey data depends on the distance to the target, the meteorological conditions and the operator. To evaluate the precision of our survey, we repeated measurements on the same points several times during each session of data acquisition. We have estimated that the uncertainty in altitude ranges between few millimeters to 1 cm, which is well within the 2σ range of the modern HLS elevation. The total station base was precisely located with an ASHTECH Zxtreme 12 GPS station.

Once the total station survey was performed, the most interesting coral microatolls (based on size, species, and complexity) were sampled with a hydraulic chainsaw. Before sampling, we placed screws along the slice axis and surveyed those screws to allow for precise positioning of the coral slice relative to sea level. We extracted coral slabs about 10 cm thick. The slabs were further reduced to 1 cm thick slices by a marble mason using a diamond wire, to be X-rayed at a hospital.

2.2. Stratigraphic Analysis and Reconstruction of the Relative Sea Level Curve

On X-rays of the coral slices, we observe an alternation of dark and light bands. Sr/Ca measurements we performed on a piece of *Siderastrea siderea* coral show that each dark/light pair of bands corresponds to 1 year of growth [*Weil-Accardo*, 2014]. On almost all X-rays, the darker band with higher aragonite density corresponds to the dry season (between December and May in the Lesser Antilles), as in Indonesian corals [*Zachariasen et al.*, 2000; *Natawidjaja et al.*, 2004] but opposite to what has been observed in Vanuatu corals [*Taylor et al.*, 1987].

Counting the growth bands from the external ring (which dates to January–February 2008) has allowed us to determine the precise timing of relative sea level fluctuations recorded in the coral skeleton. To insure our counting, we performed U/Th dating at CEREGE in Aix-en-Provence (see Appendix A). Uncertainties in our visual counting were estimated by developing a new computing method based on variations in gray scale on X-rays (see Appendix B and Figures S1 and S2 in the supporting information). On average, we estimated the 2σ uncertainties in our counting to be around $\pm$2 years, $\pm$3.5 years, $\pm$5 years, and $\pm$6 years for annual bands that are 50, 100, 150, and 200 years old, respectively [*Weil-Accardo*, 2014].

By plotting the altitude of each growth band relative to that of the external younger ring, we were able to reconstruct the history of relative sea level change recorded by the coral. We distinguished HLS and HLG (for "highest level of growth") [*Zachariasen*, 1998; *Zachariasen et al.*, 1999, 2000; *Meltzner et al.*, 2010]. HLS is the theoretical limit above which any living coral would have died due to exposure [*Meltzner et al.*, 2010], whereas the term "HLG" is used for years where HLS is not attained and corresponds to the highest level to which a coral head can grow when its growth is limited only by its natural growth rate [*Meltzner et al.*, 2010]. For HLG, the distance to the theoretical coral HLS is an unknown amount [*Meltzner et al.*, 2010].

The coral growth is often disrupted with sudden centimetric emergence events, called "die downs" [*Taylor et al.*, 1987; *Zachariasen et al.*, 1999]. Following such die downs, it is appropriate to use "HLS", while the term "HLG" is used for years not immediately following a die down [*Meltzner et al.*, 2010].

We observed that certain die downs strikingly correlate with changes in basal topography of the coral microatolls. This was also documented in coral microatolls from Indian and Pacific Ocean and can be induced by erosion or compaction of the substrate [*Scoffin et al.*, 1978; *Zachariasen*, 1998; *Zachariasen et al.*, 2000]. Together with the die downs, these additional marks on the base of a coral microatoll typify the morphology of the microatoll.

Details about the difference between HLS and HLG and about relative sea level trends inferred from the growth history are given in the supporting information (Text S1 and Figure S3). In the rest of the paper, all uncertainties are 2σ unless otherwise specified.

3. Results

3.1. Reef Complex of Martinique Island and Sampling Sites

Martinique Island is about 65 km long and 35 km wide (Figure 1b). The active volcano (Mount Pelée) dominates the morphology of the northern part of the island (Figure 1b). The island is surrounded by a reef complex

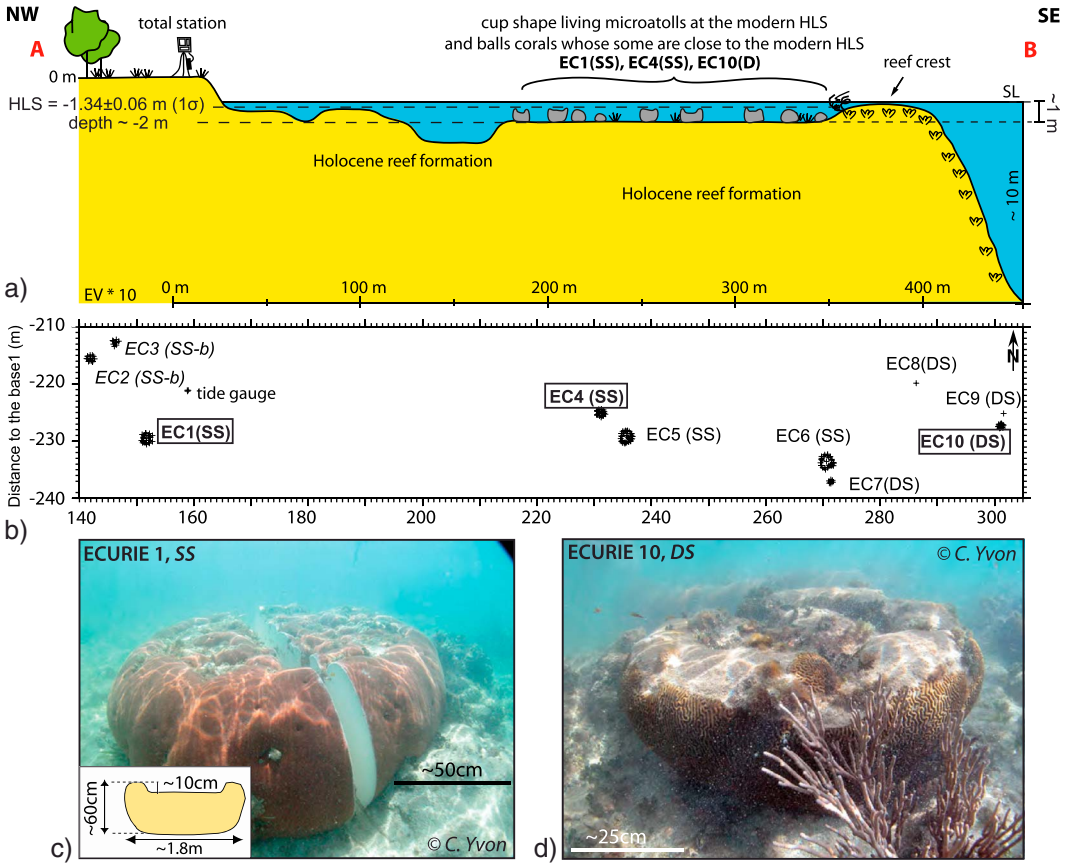

Figure 2. Example of the Pointe Ecurie site. (a) Bathymetric and topographic (data as in Figure 1c) profile of the site, from the northwest coast to the fringing reef southeast (location in Figure 1c). (b) Map view of the total station survey. Black crosses: mapped corals. EC1, EC4, and EC10 were sampled (black boxes). SS: *Siderastrea siderea* species. DS: *Diploria strigosa* species. SS-b: SS with hemispherical growth. (c) Ecurie 1 (*Siderastrea siderea*) underwater picture. Inset: sketch of the coral's cup shape. (d) Ecurie 10 (*Diploria strigosa*) underwater picture.

of Quaternary age [*Leclerc et al.*, 2015] (Figure 1b). This shallow insular plateau, ranging in depth between 0 m and 70 m, is well developed on the east side of the island, up to 25 km wide. On the west side, likely because of the activity of Mount Pelée, the insular plateau is narrow and disappears near the volcano [*Leclerc et al.*, 2015] (Figure 1b).

Our study is focused on the Atlantic side where numerous Holocene fringing reefs are found along the coast, while barrier reefs can be observed far offshore (Figures 1b and 1c).

South of the Caravelle peninsula, the coastline is irregular with numerous quiet bays connected to the open ocean. We identified numerous massive coral microatolls in such bays. Three sites were explored and sampled in Robert and Galion Bays, which are located about 250 km from the accretionary prism deformation front. The three sites are fringing reefs, developed between 0 m and 10 m depth, while both bays are up to 20 m deep (Figures 1c–1e).

"Pointe Ecurie" is the first site we sampled. It sits in Robert Bay between Pointe Ecurie and Chancel islet (Figures 1c and 1d). The second site, "Chancel islet," is located south of Chancel islet, 1 km east of the "Pointe Ecurie" site (Figures 1c and 1d). Finally, the last site, "Gros Raisins," is 4 km northeast of "Pointe Ecurie," located in the Gros Raisins Bay in the eastern part of Galion Bay (Figures 1c and 1e).

Among the six living microatolls we sampled, five are *Siderastrea siderea* species and one is *Diploria strigosa* species (Figures 2c and 2d). The growth rate of the former species has been estimated at about 5 mm/yr with geochemical analysis and band counting [*Weil-Accardo*, 2014], whereas the second species grows at about 1 cm/yr according to band counting [*Weil-Accardo*, 2014]. All coral microatolls we studied displayed a cup shape (Figures 2c and 2d), characteristic of a submergence setting [*Taylor et al.*, 1987].

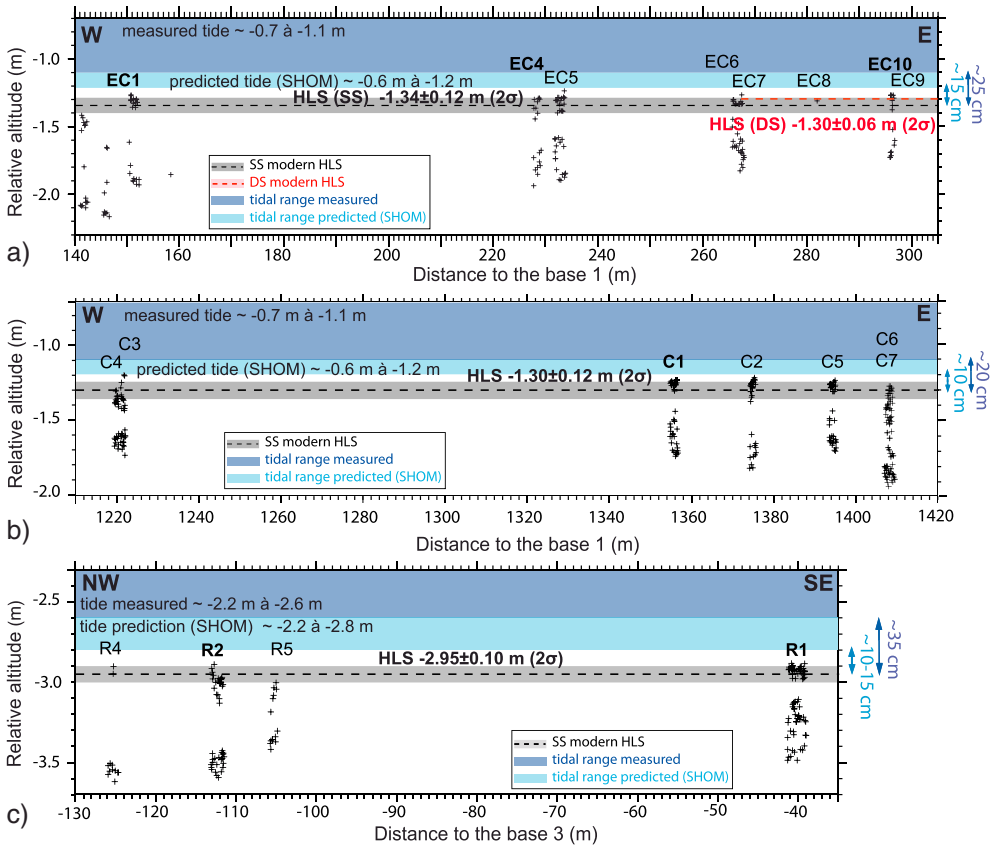

Figure 3. HLS elevations of the sampling sites (profiles across the sites). Vertical axis: elevation relative to that of the total station base. Horizontal axis: distance to the base. Black crosses: measurements of the coral base, the center of the coral, and the top of external living rim (HLS measurements). All points are projected along a N90° profile. The top of the external rim of the microatolls marks the modern HLS of the area. SS: *Siderastrea siderea* species. DS: *Diploria strigosa* species. EC1, EC4, EC10, C1, R1, and R2 indicate sampled corals. (a) Pointe Ecurie area. (b) Chancel islet. (c) Gros Raisins Bay.

3.2. Site Descriptions, Modern HLS Elevations, and Relationship With Tidal Range

For the three sites we explored, coral microatolls were found in a shallow lagoon (between 0.5 m and 2 m depth), on a mainly sandy substrate (Figure 2a, Text S2 and Figures S4 to S8 in the supporting information). The lagoon is bounded offshore by the reef crest, beyond which, in the buttress zone, the depth increases suddenly to 10 m within about 50 m distance (Figure 2a).

At Pointe Ecurie, we mapped eight living coral microatolls (four are *Siderastrea siderea* and four are *Diploria strigosa*) within a 160 m by 30 m area (Figure 2b). The tops of the living rims of these eight microatolls we surveyed indicate the modern HLS at -1.34 ± 0.12 m for *Siderastrea siderea* and at -1.30 ± 0.06 m for *Diploria strigosa* (altitudes relative to the height of the total station) (Figure 3a). At the scale of the whole site, the HLS of *Diploria Strigosa* is hence slightly higher (up to 4 cm) than that of *Siderastrea siderea* (Figure 3a). Small variations in HLS elevation of coral from different species have also been documented in Indonesia [*Natawidjaja et al.*, 2006; *Meltzner et al.*, 2006; *Briggs et al.*, 2006; *Meltzner*, 2010; *Meltzner et al.*, 2010]. Among the mapped corals, two *Siderastrea siderea* specimens (Ecurie 1/EC1, Ecurie 4/EC4) and one *Diploria strigosa* specimen (Ecurie 10/EC10) were sampled.

Seven *Siderastrea siderea* microatolls were surveyed at Chancel islet within a 200 m by 120 m area (Figure S4c). Only one (Chancel 1/C1) was sampled (Figure S4). As the total station bases of the two sites, Pointe Ecurie and Chancel islet, have been connected via survey (Figure 1d), all measurements have been referenced to the Pointe Ecurie base. The modern HLS of *Siderastrea siderea* at the Chancel islet site lies at -1.30 ± 0.12 m of altitude compared to the total station base at Pointe Ecurie (Figure 3b). The modern HLS is consistent between the two sites, which are separated by more than 1 km.

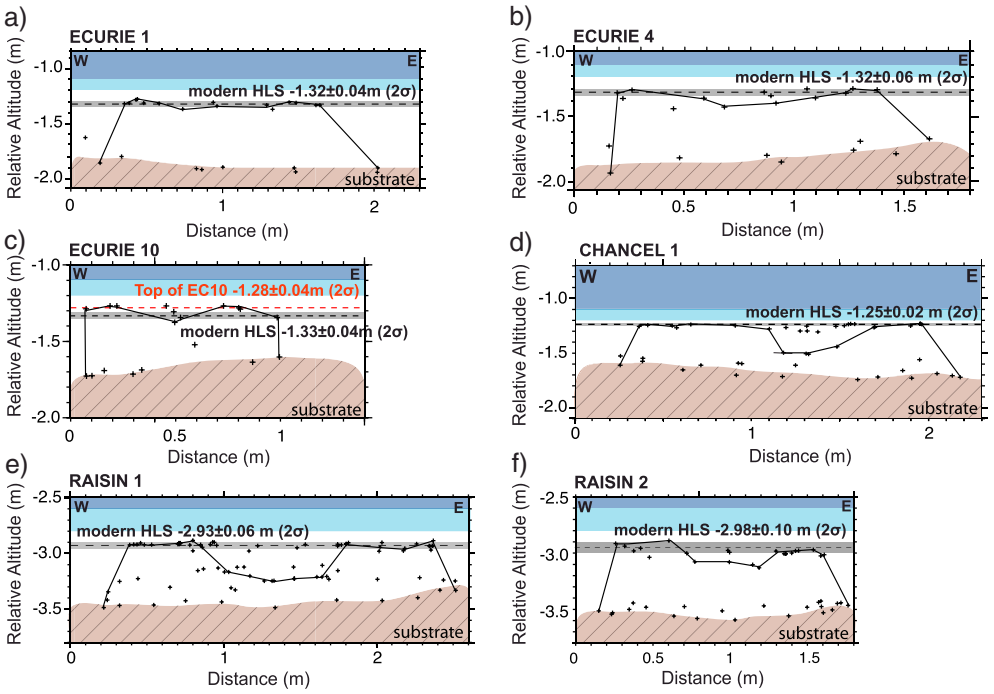

Figure 4. HLS elevations of sampled corals (profiles across the corals). Vertical axis and black crosses as in Figure 3. All points are projected in a N90° direction. Maps are in Figure S18. Dashed black lines and gray rectangles: modern HLS usually corresponding to the top of the coral (except for Ecurie 10 whose top is drawn with a dashed red line, see main text). In brown: coral substrate. (a) Ecurie 1. (b) Ecurie 4. (c) Ecurie 10. A picture of Ecurie 10 (with its dead top and its outermost living rim highlighted) is given in Figure S16a in the supporting information. (d) Chancel 1. (e) Raisin 1. (f) Raisin 2.

At Gros Raisin Bay, we mapped four *Siderastrea siderea* microatolls within a 90 m by 80 m area (Figure S5c) and sampled two of them (Raisin 1/R1 and Raisin 2/R2). The modern HLS lies at -2.95 ± 0.10 m of altitude compared to the total station base of the site (Figure 3c). It was not possible to connect the total station base at this site to the bases of the two previous sites.

The modern HLS levels of individual sampled microatolls are consistent with that of neighboring microatolls (Figure 4) and have uncertainties of a few centimeters (up to 10 cm for Raisin 2, because its HLS was measured on discontinuous small colonies instead of on one continuous living rim, Figure 4f). The top rim of the *Diploria strigosa* specimen (Ecurie 10) lies at -1.28 ± 0.04 m of altitude relative to the total station base (Figure 4c) but died recently. Its modern HLS in 2008 was about 5 cm lower (-1.33 ± 0.04 m), similar to that of the neighboring *Siderastrea siderea* corals (Figure 4c).

Tides were measured during fieldwork (at the three sites between 30 January 2008 and 7 February 2008) and compared to the SHOM (Hydrographic and Oceanographic Department of the French Navy) predictions at Le Robert (Text S3 and Figure S9 in the supporting information). Despite uncertainties and limitations of the SHOM predictive tide model (Text S3), the good agreement between our observations and the predictions at the time of our water level measurements make us confident in using this simplified SHOM tidal model to link our HLS measurements to the complete tide cycle (outside the range of our direct water level measurements). According to the SHOM predictions, during our fieldwork, the coral microatolls from the three studied sites were never exposed since they were about 10–15 cm below the daily low tides during that time (Figure 3 and S9a). For the whole of 2008, the SHOM tide model predicts a maximum tidal range of 85 cm at Le Robert, and the 2008 HLS lies about 5 cm below the predicted lowest tide in 2008 (Figure S9b). The corals would be more vulnerable in spring (from April to June) when lowest tides occurred in the daytime between 9:00 A.M. and 1:00 P.M (Figure S9b).

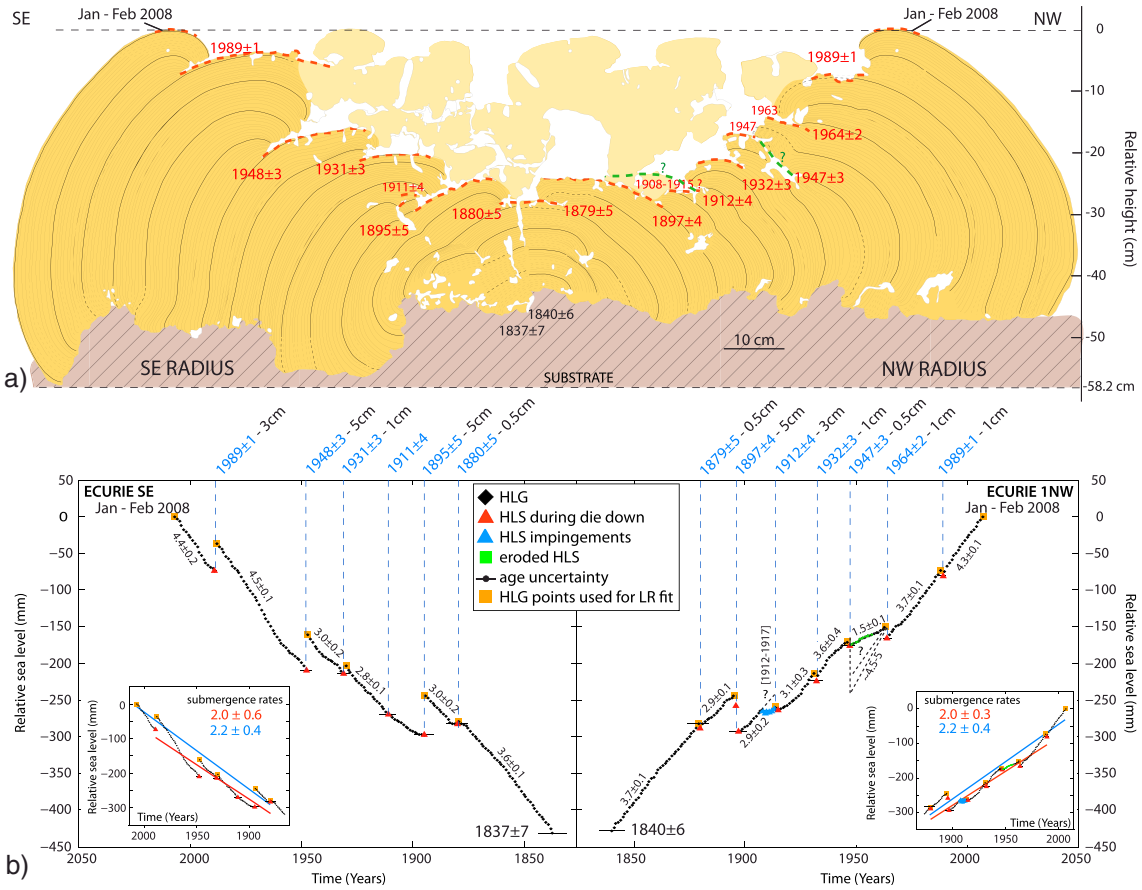

Figure 5. Slab stratigraphy of Ecurie 1. (a) Location of the slab in Figure S18a. In yellow: coral skeleton with holes in white. Annual growth bands in black with thicker bands every 10 years. Dashed black lines: unclear bands. As the external ring dates to January–February 2008, each growth band corresponds to the beginning of the year. New growths colonizing the center of the coral are in lighter yellow. Dashed red lines with corresponding dates: die downs. Dashed green lines: possible larger die downs on the northwest radius. Brown area: substrate. (b) HLS curve of Ecurie 1. From the drawing, we plot the upper altitude of each growth band. The reference altitude (0) is the elevation of the 2008 growth band. The HLS curves have been constructed for each radius and positioned relative to each other. Dashed blue lines: die down events with dates indicated in blue and amplitudes of the relative sea level drops in black. Numbers in black with uncertainties between die downs: upward coral growth rates (given in millimeters per year with 2σ uncertainties) calculated with linear regression. Horizontal error bars added for a few HLS points indicate the uncertainty in growth band counting, estimated with the computing method described in Appendix B. Inset: red and blue straight lines: Submergence rates (given in millimeters per year with 2σ uncertainty) calculated by linear regression (LR) from HLS points only (blue and red triangles) [*Zachariasen*, 1998; *Zachariasen et al.*, 2000] or with HLG points preceding die downs (orange squares) [*Meltzner et al.*, 2010], respectively.

This comparison between the modern HLS and the tidal cycle implies that coral microatolls from the three sites were recording modern HLS at similar elevation in 2008 (this is especially important for the Gros Raisin Bay whose measurements were not referenced to the Pointe Ecurie base), and they can be used as natural tide gauges.

3.3. Coral Slab Stratigraphy

In this section, we describe the detailed slab stratigraphy of two corals: Ecurie 1, sampled along a diameter, and Raisin 1 which is the oldest one. Complete descriptions of other corals, pictures, and X-ray of corals are given in the supporting information (Text S4 and Figures S10 to S17).

3.3.1. Ecurie 1

Ecurie 1 is a 1.80 m wide and 0.6 m high *Siderastrea siderea* microatoll (Figure 4a). It has a clear cup shape, partially hidden by numerous new growths in its center (Figure 5a).

Ecurie 1 began to grow freely in every direction in 1837 ± 7 until it first experienced a small die down of 0.5 cm of amplitude around 1879±5 (NW radius) to 1880±5 (SE radius) (Figure 5a). During this stage of growth, which lasted more than 40 years, the coral adopted a flattened ball shape suggesting a shallow water environment (Figure 5a). Along the southeast radius, other die downs occurred in 1895 ± 5, 1911 ± 4, 1931 ± 3, 1948 ± 3,

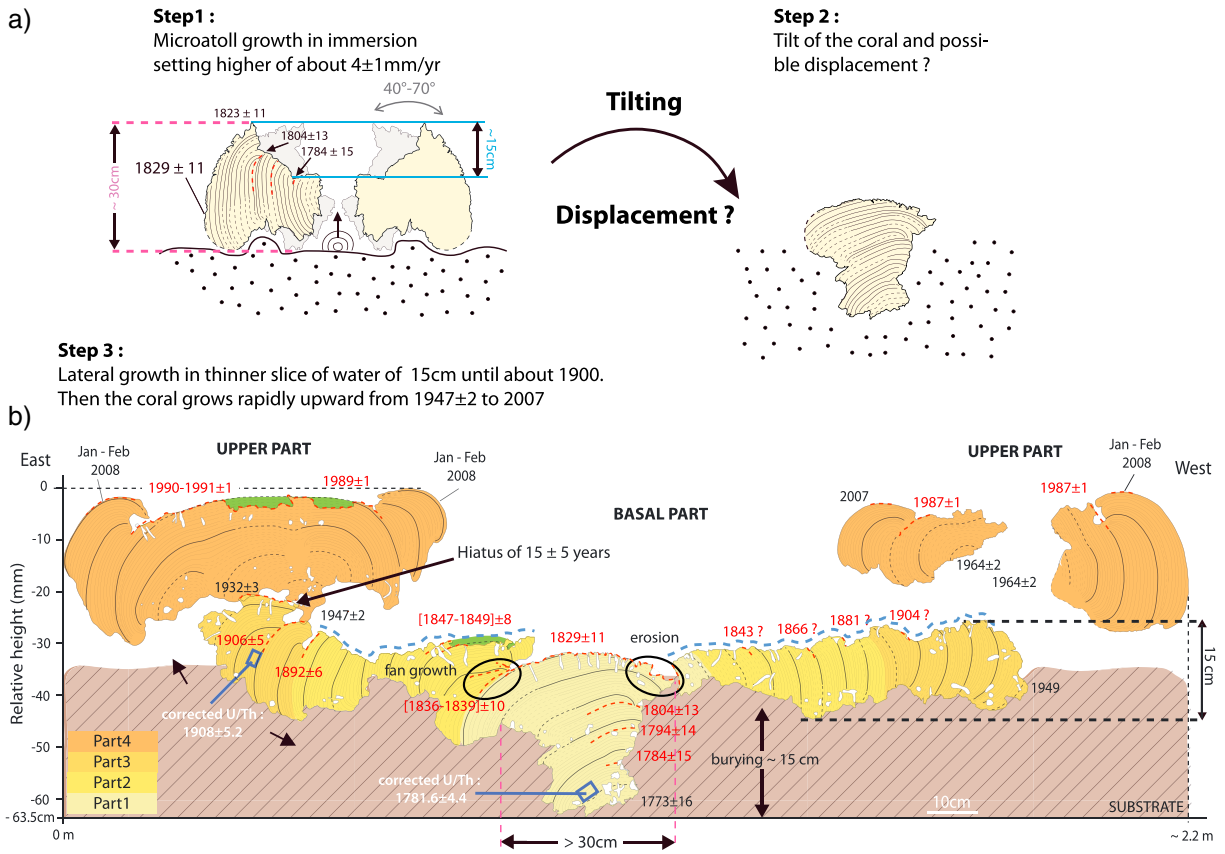

Figure 6. a) History of Raisin 1. Step 1: Raisin 1 had a microatoll shape and was growing in a submergence setting until 1823 ± 11. Step 2: A broken piece of Raisin 1 was tilted westward (about 40°-70°, Figure S12c) and three quarters of this piece was buried by sand. Step 3: Raisin 1 grew outward and developed a large 15 cm-thick plateau. After the tilting, the deeper east side grew faster forming a fan, while the west side, probably shallower, was eroded. The coral continued its growth with increases in submergence rate around 1892 ± 6 and 1947 ± 2. The estimation of the tilting between the steps 1 and 2 was done by using the orientation of die downs (Figure S12), and the curvature of the non-eroded growth bands between 1804 ± 13 and 1819 ± 12. We infer several possibilities (Figure S12) (light yellow and light grey drawing in step 1). The growth bands between 1824 ± 11 and 1829 ± 1 were too eroded to include in the submergence rate calculation. b) Slab stratigraphy of Raisin 1. Symbols and dates as in Figure 5. Dashed blue lines: partly eroded areas upper surface with reconstruction (green area where the remaining upper parts were previously connected). Blue squares: U/Th sample locations with dates and uncertainties in white (Table 1). Dates in black: beginning of growth and major morphological changes. The counting on the west radius is based on the one performed on the east radius (more preserved and continuous record). Dates in red: die downs (less clear on the western radius where only possible residual HLS impingements are found). Orange color scale used to differentiate the four stages of growth of Raisin 1 (see text).

and 1989 ± 1, with amplitudes of 5 cm, <0.5 cm, 1 cm, 5 cm, and 3 cm, respectively (Figure 5). Along the northwest radius, die downs occurred at the same times with equal or lower amplitudes, and one very small (1 cm in amplitude) additional event occurred in 1964 ± 2 (Figure 5a). We must note that the amplitudes of the 1912 ± 4 and 1947 ± 3 events were difficult to estimate on the northwest portion because the X-ray is less clear in that area (Figure 5).

Table 1. Results of Uranium-Thorium Dating of Coral Microatolls Raisin 1 and Raisin 2[a]

Sample Name	AD Raw date (±2σ)	AD Corrected date (±2σ)	$[^{238}U]$ (ppb) (±2σ)	$[^{234}U/^{238}U]$ (±2σ)	$[^{234}U/^{238}U]_i$ (±2σ)	$[^{238}U/^{232}Th]$ (±2σ)
Raisin 1-1	1771.1 (±3.7)	1781.6 (±6.4)	2614 (±4)	1.147 (±0.002)	1.147 (±0.002)	11781 (±34)
Raisin 1-2	1896.2 (±4.3)	1908.0 (±7.2)	2285 (±3)	1.1470 (±0.0007)	1.1470 (±0.0007)	10578 (±30)
Raisin 2	1880.1 (±4.1)	1886.6 (±5.2)	2142 (±3)	1.1460 (±0.0006)	1.1470 (±0.0006)	38159 (±123)

[a]Correction of the detrital thorium component has been done assuming a detrital ratio ($^{230}Th/^{232}Th$) of 1.30 ± 0.65 for Raisin 1-1 and Raisin 1-2 and 2.6 ± 1.3 for Raisin 2 (see Appendix A). These values for the nonradiogenic thorium component were calculated based on other Martinique samples of known age (see Appendix A).

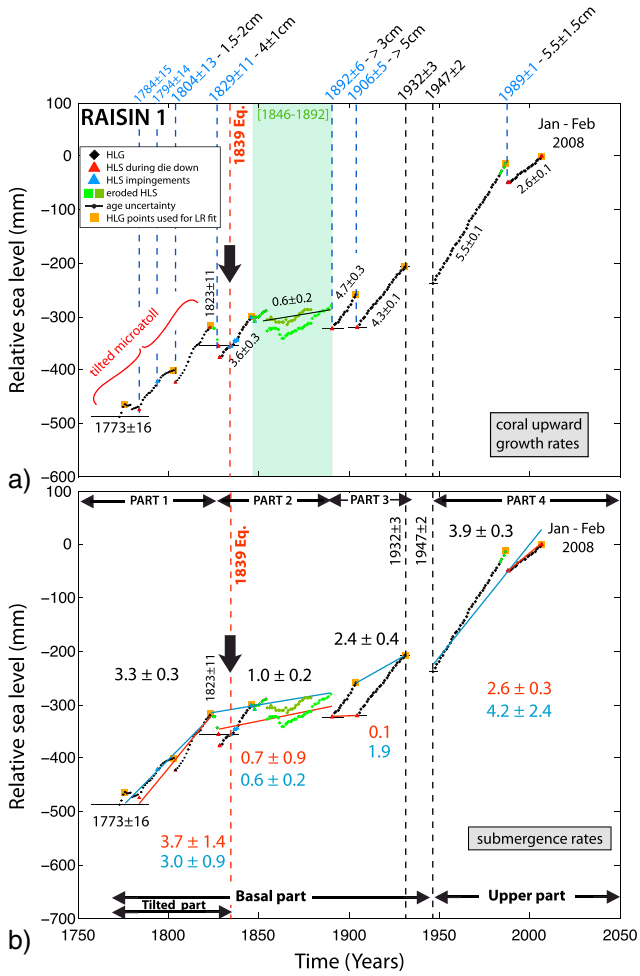

Figure 7. Raisin 1 HLS curve. Symbols, rates, and dates as in Figure 5. (a) Most of the HLS curve (black dots and light green squares) was based on the east radius, with the exception of the growth bands between 1856 and 1883, which were better preserved on the west radius (dark green squares) (Figure 6b). Green band: erosion period between 1846 and 1892. Dashed red line: 1839 earthquake. Black arrow: major change in morphology corresponding to the plateau development. Before 1829 ± 11: HLS points measured on the tilted part with a tilt correction of 70° (Figures 6a and S12c; see text). (b) Symbols, rates, and dates as in Figure 5. Numbers in black: submergence rates deduced by using all HLS and HLG points between 1784 ± 15 and 1823 ± 11; between 1829 ± 11 and 1892 ± 6, between 1892 ± 6 and 1932 ± 3, and between 1947 ± 2 and 2008 [*Zachariasen*, 1998; *Zachariasen et al.*, 2000]. Before 1829 ± 11: submergence rate, corrected for a tilt of 70°, estimated by using growth bands between 1784 ± 15 and 1823 ± 11 (those between 1824 ± 11 and 1829 ± 11 being too eroded). The different periods of growth (Parts 1–4; see text) are symbolized with black arrows.

Similar to die down amplitude (which varies by a few centimeters between the two radii), we also observed small differences in upward growth rate between the two radii (a few tenths of a millimeter per year) (Figure 5b). These small stratigraphic differences are within the precision range of the modern HLS, and are probably simply an expression of the natural variability of coral growth in response to relative sea level changes.

Over 130 years, Ecurie 1 recorded a submergence rate between 2.0 ± 0.6 mm/yr for the SE radius (±0.3 for the NW radius) and 2.2 ± 0.4 mm/yr, depending on the calculation method we used (inset in Figure 5b). The upward growth rates (with an average rate of 3 mm/yr) have always been lower than the maximal growth rate of the species (about 5 mm/yr), except for the last four to six decades. Indeed, during the latter period, upward growth rates have been higher (reaching more than 4 mm/yr) (Figure 5b). This is associated with a clear change in morphology and a decrease in the frequency of die downs starting in 1947–1948 (Figure 5a).

3.3.2. Raisin 1

Raisin 1 is 2.20 m wide and 0.6 m high (Figure 4e). It is the largest *Siderastrea siderea* microatoll we sampled in Martinique. Unlike the rounded perimeter observed for other microatolls (Figures S18a–S18d and S18f), Raisin 1 has a horseshoe shape (Figures S11a and S18e). A double rim with a dead central part sits on the top of a large asymmetric basal plateau (Figures 6, S11, and S18e). This basal plateau is partially eroded, encrusted by numerous microorganisms, and partly buried by sand (Figure 6).

We dated the east radius of the plateau with the TIMS U/Th method in two places (Figure 6). One sample was taken at the base of the coral, while the second one was sampled close to the transition between the basal plateau and the rim. After correction of the nonradiogenic thorium component (see Appendix A), we obtained a date of A.D. 1781.6 ± 4.4 for the first sample and A.D. 1908 ± 5.2 for the second one (Table 1 and Figure 6). According to the U/Th dating, Raisin 1 began to grow in 1773 ± 16 and recorded two major die downs in 1892 ± 6 and 1906 ± 5 (Figure 6). Both die downs are consistent with those recorded in 1895 − 1897 ± 5 and in 1911–1912 ± 4 by Ecurie 1 (Figure 5). Since the upper part began to grow in 1947 ± 2 and the basal part stopped growing in 1932 ± 3 (Figure 6), this indicates a gap of 15 ± 5 years between the two parts of the coral.

The HLS curve has been mainly constructed based on the better preserved eastern radius, except for the period between 1856 and 1883. The coral morphology indicates a development in four steps (Figures 6 and 7).

1. Between 1773 ± 16 and 1829 ± 11, the basal part of Raisin 1 (Part 1) has downward tapering morphology (Figure 6) contrasting with Ecurie 1 and all described microatolls (Text S4 in the supporting information). It is clearly a microatoll that was tilted westward (Figure 6a). This is commonly observed among coral microatolls that can be dislodged, overturned, or tilted by storms, earthquake ground shaking, or tsunamis [e.g., *Scoffin et al.*, 1978; *Meltzner et al.*, 2010]. The morphology of Part 1 is marked by residual die downs, particularly clear on the X-ray, in 1784 ± 15, 1794 ± 14, and 1804 ± 13, as well as clear changes in the basal topography of the coral (Figures 6a and S12b). These residual die downs are nearly horizontal, in contrast to other die downs observed on Parts 2 to 4 (Figures 6 and S12a). The range in dip (25° to 50°, Figure S12a) of the main die downs that occurred after 1829 ± 11 (Parts 2 to 4) is a strong indicator to restore the original position of Part 1 with an eastward tilt ranging between 40° and 70° (Figures 6a and S12c). By considering an eastward tilt of 70°, we calculate a mean submergence rate of 3.5 ± 1 mm/yr between 1784 ± 15 (first preserved HLS impingement) and 1823 ± 11 (Figure 7 and Table 2). After this period, another large die down (4 ± 1 cm) occurred in 1829 ± 11 (Figure 6b). Following 1829 ± 11, the coral was tilted, possibly displaced, and buried by sand (Figure 6). Then it continued to grow laterally between 1829 ± 11 and 1932 ± 3 and developed its plateau (Parts 2 and 3, Figure 6b), which contrasts with the setting of rapid sea level rise recorded by the coral before 1829 ± 11 (Part 1).
2. Between 1829 ± 11 and 1892 ± 6 (Part 2) Raisin 1 recorded nearly stable relative sea level with a submergence rate lower than 1 mm/yr (Figure 7b). This part corresponds to a flat plateau, partially eroded with likely residual die downs (Figure 6b). Part 2 is half as thick vertically than Part 1 (Figure 6b). This implies that Part 2 developed in a much shallower water column than Part 1, either because the tilted portion was displaced into a shallower area of the bay and/or because the relative sea level decreased. Owing to the tilting, the coral was able to grow rapidly on the eastern side between 1829 ± 11 and 1838 ± 10, with growth bands forming a fan, whereas the western part was eroded (Figure 6b). This is probably because the eastern side was under the water whereas the western part was emergent.
3. After 1892 ± 6, we observe a change in the morphology of Raisin 1, with a better preservation of the upper surface of the coral and faster upward growth rates (Part 3) (Figures 6b and 7a). During this period, upward growth rates reached 4 mm/yr (Figures 6b and 7a), two major die downs occurred in 1892 ± 6 and 1906 ± 5 with 3 cm and >5 cm amplitude, respectively (Figures 6b and 7a), and the submergence rate increased up to 2.4 ± 0.4 mm/yr (Figure 7b and Table 2).
4. The upper part of Raisin 1 (Part 4) began to develop in 1947 ± 2. It corresponds to the upper rim of the coral (Figure 6b). From this date, the coral grew continuously upward at the rate of 5.1 ± 0.1 mm/yr until it recorded a die down in 1989 ± 1 of 5.5 ± 1.5 cm amplitude (Figures 6b and 7a). After this event, the coral continued growing upward at a slower rate (2.6 ± 0.1 mm/yr) (Figures 6b and 7a). We calculated that during the last six decades, Raisin 1 recorded an average submergence rate of about 4 mm/yr (Figure 7b).

Table 2. Submergence Rates (in Millimeters Per Year With 2σ Uncertainties) Recorded by Coral Microatolls, Calculated With Different Methods: *Zachariasen* [1998], *Zachariasen et al.* [2000], and *Meltzner et al.* [2010][a]

Sample name	Zach-1	Zach-2	Zach-3a	Zach-3b	Meltzner
Ecurie1 SE	2.0 ± 0.6	2.3 ± 0.1	2.2	1.9	2.2 ± 0.4
(1880–2008)	$r^2 = 0.9143$	$r^2 = 0.9345$			$r^2 = 0.9761$
Ecurie1 NW	2.0 ± 0.3	2.2 ± 0.1	2.3	1.9	2.2 ± 0.4
(1879–2008)	$r^2 = 0.9285$	$r^2 = 0.9366$			$r^2 = 0.9424$
Ecurie4	2.0 ± 0.4	2.1 ± 0.1	2.1	1.7	2.0 ± 0.2
(1879–2008)	$r^2 = 0.9464$	$r^2 = 0.9655$			$r^2 = 0.9864$
Ecurie10 E	1.7 ± 1.9	2.1 ± 1.2	—	1.7	3.1 ± 3.2
(1977–2008)	$r^2 = 0.5996$	$r^2 = 0.3184$			$r^2 = 0.6466$
Ecurie10 W	1.5 ± 2.0	1.6 ± 1.1	—	1.7	1.8 ± 2.3
(1977–2008)	$r^2 = 0.3595$	$r^2 = 0.2342$			$r^2 = 0.3770$
Chancel1	2.0 ± 0.3	2.4 ± 0.1	2.4	2.1	2.3 ± 0.1
(1881–2008)	$r^2 = 0.9311$	$r^2 = 0.9492$			$r^2 = 0.9975$
Raisin1 Part 1	3.7 ± 1.4	3.3 ± 0.3	—	3.9	3.0 ± 0.9
(1784–1823)	$r^2 = 0.9295$	$r^2 = 0.9211$			$r^2 = 0.9762$
Raisin1 Part 2	0.7 ± 0.9	1.0 ± 0.2	1.2	0.5	0.6 ± 0.2
(1829–1892 ± 6)	$r^2 = 0.2594$	$r^2 = 0.6325$			$r^2 = 0.9357$
Raisin1 Part 3	0.1[b]	2.4 ± 0.4	2.9		1.9
(1892 ± 6–1932)		$r^2 = 0.7734$			
Raisin1 Part 4	2.6 ± 0.3	3.9 ± 0.3	4.0	4.5	4.2 ± 2.4
(1947–2008)	$r^2 = 0.9978$	$r^2 = 0.9294$			$r^2 = 0.9231$
Raisin2	3.0 ± 1.4	3.0 ± 0.2	3.7	3.5	2.7 ± 0.5
(1914–2008)	$r^2 = 0.8676$	$r^2 = 0.8737$			$r^2 = 0.9840$

[a]Calculations with the only HLS points (Zach-1), all HLG and HLS points starting from the first HLS (Zach-2), the difference between the first HLS and the 2008 HLS or HLG (Zach-3a), and the difference between the first HLS and the last HLS (Zach-3b) [*Zachariasen*, 1998; *Zachariasen et al.*, 2000]. For the Zach-3 method, the trend is calculated using only two points, which does not permit an uncertainty calculation. For this method, we have distinguished two cases. In the first case, we considered every 2008 elevation (HLS or HLG). In the second case, we considered only the last HLS. For almost all samples, the total submergence rate is close to other rates calculated by taking into account the 2008 elevation. This confirms that the difference between the HLG and HLS in 2008 is small. *Meltzner et al.* [2010]: calculation method based on the noneroded HLG immediately prior to the die downs (except the first one).

[b]For the stage 3 of Raisin 1, the rate calculated with the only HLS points (Zach-1) is not consistent with other rates, because only two HLSs points that have similar altitude were recorded over that period of growth. This makes this rate unreliable.

3.3.3. Other Corals (Ecurie 4, Chancel 1, Raisin 2, and Ecurie 10)

The width of the remaining corals ranges between 1 m and 2 m and all are 0.5–0.6 m high (Figures 4b–4d and 4f). They also display pronounced cup shapes, sometimes hidden by new growths that have colonized their centers (Figures 8–11).

Siderastrea siderea corals recorded submergence at rates ranging between 2.0 ± 0.2 mm/yr and 3.0 ± 1.4 mm/yr (Figures 8b, 9b, and 10b).

The *Diploria strigosa* microatoll Ecurie 10, which is the shortest record and the most affected by die downs, recorded submergence at a rate ranging between 1.5 ± 2.0 mm/yr and 3.1 ± 3.2 mm/yr (Figure 11b), consistent with those calculated for *Siderastrea siderea* corals.

The die down chronologies of Ecurie 4 (Figure 8) and Chancel 1 (Figure 9) are consistent with that of Ecurie 1. The upward growth of Ecurie 4 was disrupted by six major centimetric die downs in 1896 ± 3, 1913 ± 3, 1928 ± 2, 1947 ± 2, 1961 ± 2, and 1989 ± 1, with amplitudes of 5.6 cm, 0.6 cm, 2 cm, 2 cm, 1.5 cm, and 3 cm, respectively (Figure 8). Chancel 1 recorded four die downs in 1881 ± 4, 1896 ± 4, 1948 ± 2, and 1989 ± 1 with amplitudes of 1.5 cm, 5 cm, 5 cm, and 2 cm (Figure 9). Although erosion partially removed the upper surface of the coral between 1927 ± 3 and 1948 ± 2 (Figure 9), a fourth event can be identified in 1931 ± 3 (Figure 9).

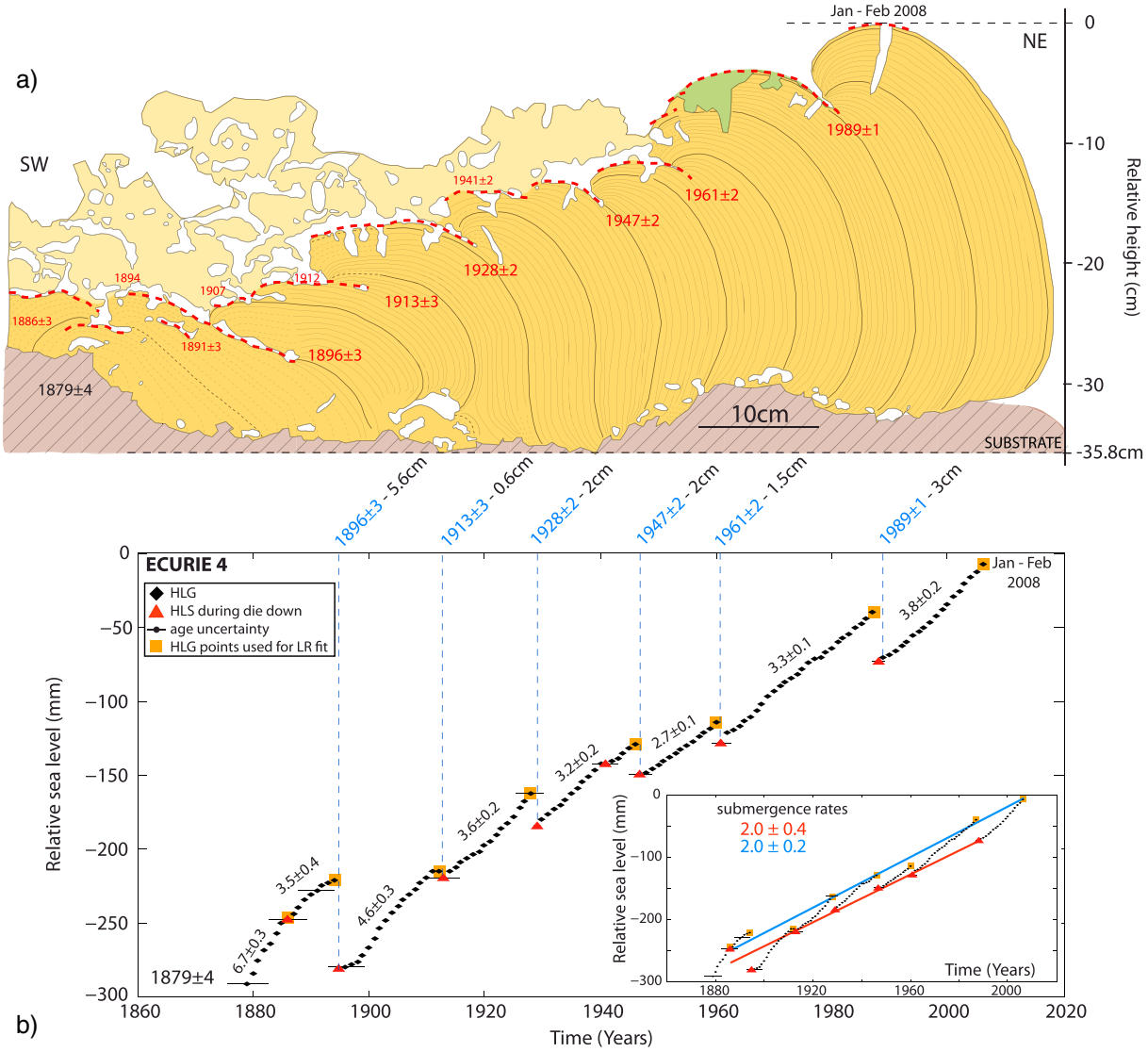

Figure 8. Slab stratigraphy of Ecurie 4. (a) Symbols and dates as in Figure 5. Green area: coral piece which was broken during the sampling and whose limits have been interpolated. (b) HLS curve of Ecurie 4. Symbols, rates, and dates as in Figure 5.

This event followed a period of slower upward growth between 1912 and 1931 (Figure 9b), characterized by a significant decrease of the band thickness toward the surface (Figure 9a).

In contrast, the die down chronologies of Raisin 2 and Ecurie 10 are not as well correlated with the those previously described. After a first impingement in 1914 ± 6 (Figure 10), Raisin 2 recorded three die downs in 1956 ± 5, 1976 ± 5, and in 1994 ± 5 with amplitudes of 1 cm, 3 cm, and 5 cm, respectively (Figure 10). Ecurie 10 recorded die downs in 1977 ± 1, 1985 ± 1, 1989 ± 1, 1996 ± 1, and 2007, with amplitudes of 1.5 cm, 3.5 cm, 5 cm, 1 cm, and 5 cm, respectively (Figure 11).

Combining all the coral records, we found evidence of a change around 1950. As was the case for Ecurie 1, the die down frequency of Ecurie 4 decreased in 1961 ± 2 from one die down every 15–20 years to one die down every 30 years. This change is associated with an increase in the coral's upward growth rates (Figure 8b). The slightly eroded and bioturbated plateau of Chancel 1, associated with a much slower upward growth rate between 1927 ± 3 and 1948 ± 2 (Figure 9), suggests that the coral was growing very close to its HLS during that time. After 1948 ± 2, the coral grew upward more rapidly at a rate of 4.5 ± 0.1 mm/yr for 40 years and developed a columnar morphology (Figure 9). This likely indicates that the water depth increased significantly after 1948 ± 2. No variation in die down frequency is observed for the shortest record Ecurie 10.

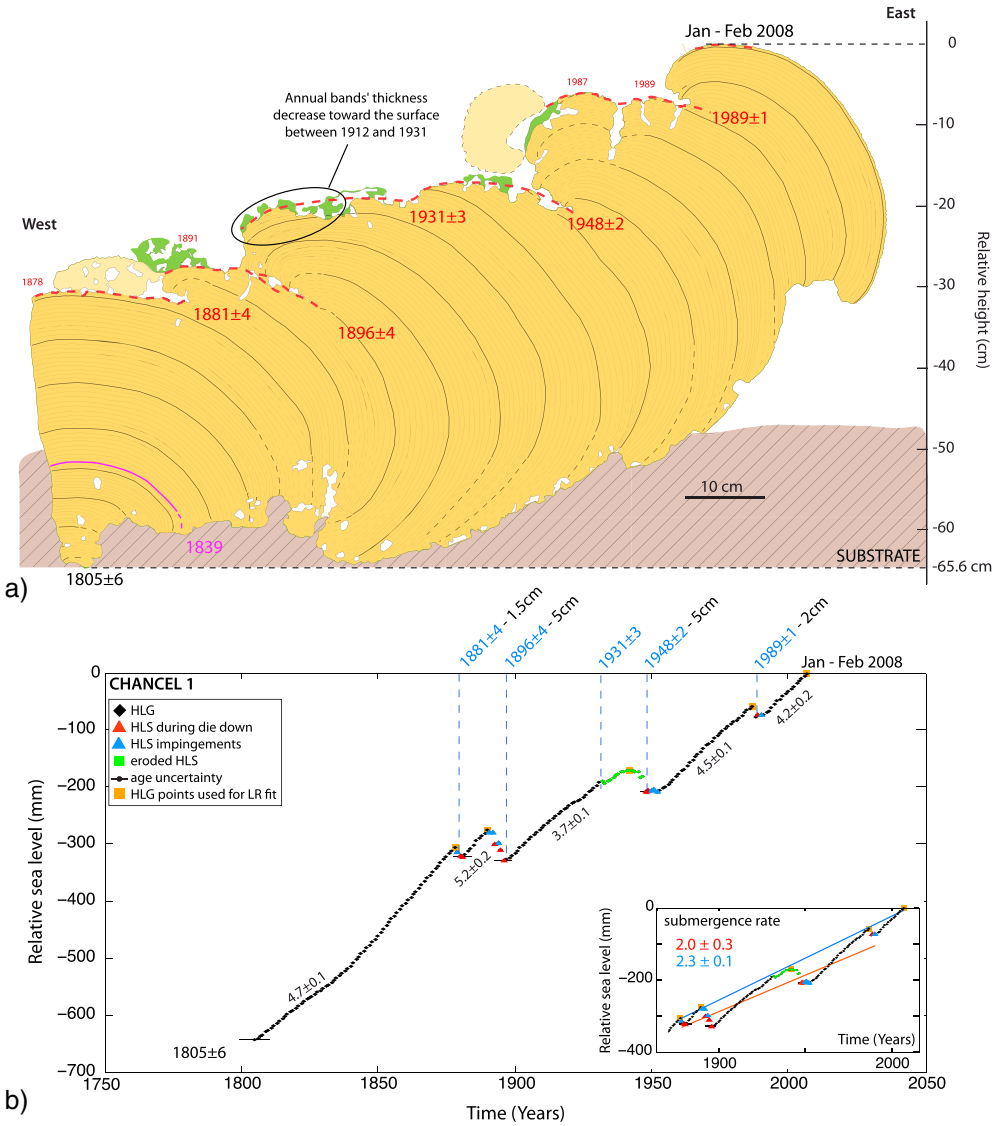

Figure 9. Slab stratigraphy of Chancel 1. (a) Symbols and dates as in Figure 5. Green area: eroded upper surface of the coral. (b) HLS curve of Chancel 1. Symbols, rates, and dates as in Figure 5.

However, Ecurie 10 grew upward by 30 cm, at about 1 cm/yr between 1948 ± 2 and 1977 ± 1 (Figure 11), which is greater than what we observed for the *Siderastrea siderea* corals Ecurie 1 and Ecurie 4 (20 cm, Figure 5 and 5 cm, Figure 8 respectively) during their periods of unconstrained growth at the beginning of their development. Moreover, Ecurie 1 and Ecurie 4 grew on deeper substrate (by 20 cm and 10 cm, respectively) than Ecurie 10 (Figures 4a–4c), implying that Ecurie 10 began to grow at a shallower depth than Ecurie 1 and Ecurie 4. Overall, these observations suggest that Ecurie 10 began to grow in a setting of rapid sea level increase. Similar to the period of unconstrained upward growth inferred from Raisin 1 and Ecurie 10, Raisin 2 grew continuously upward between 1914 ± 6 and 1956 ± 5 (Figure 10).

3.4. Submergence Rates

The submergence rates we calculate are almost identical regardless of the method we used, except for the shortest records of Ecurie 10 and Raisin 1 Parts 3 and 4 (Table 2). This is in agreement with the test we performed in the supporting information (Text S1), using the calculation methods of *Zachariasen* [1998], *Zachariasen et al.* [2000], and *Meltzner et al.* [2010] (Figure S3). Only the uncertainties fluctuate as a function of the number of data points used for the linear regression (Table 2). The use of numerous methods is a good way to evaluate the signal robustness.

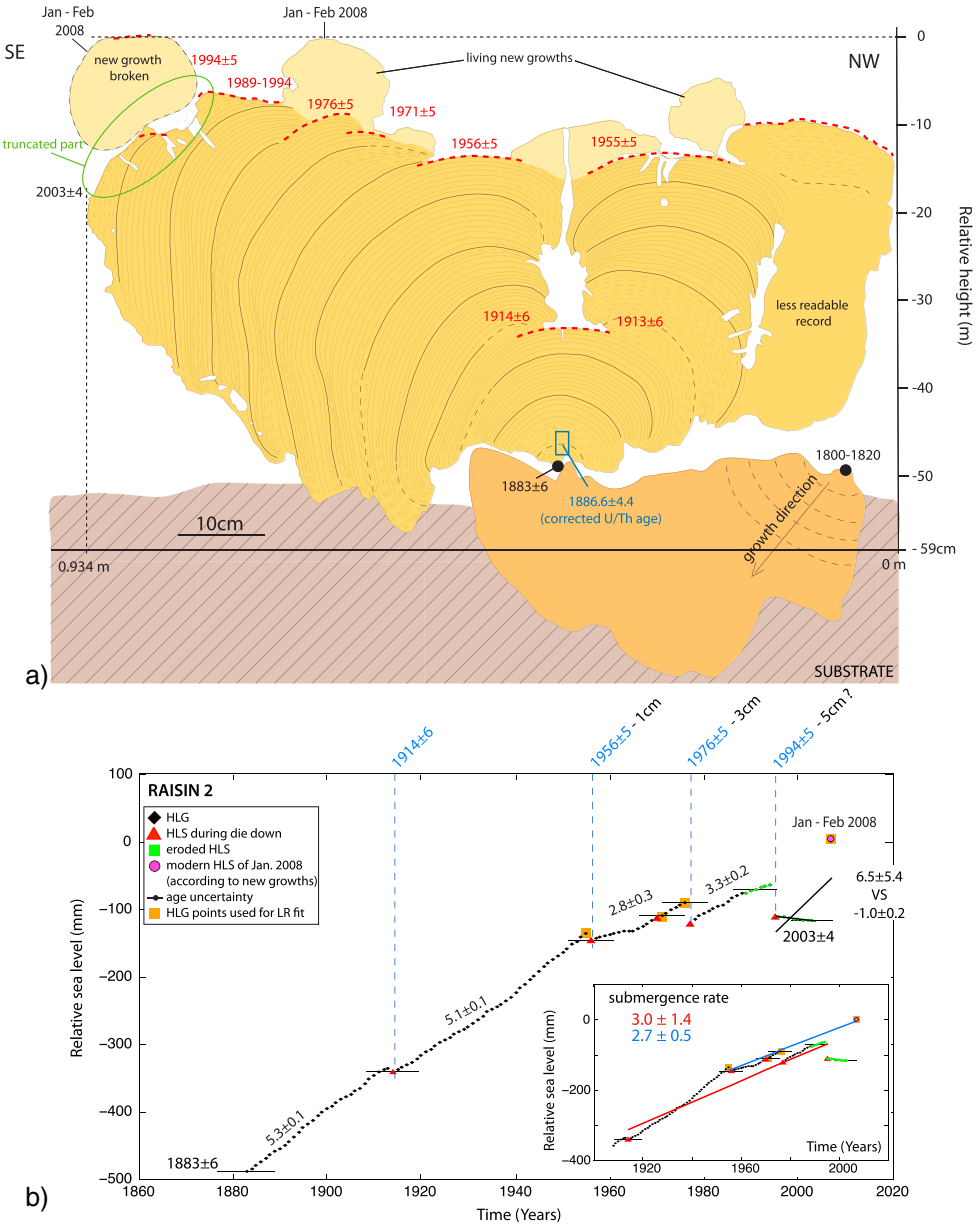

Figure 10. Slab stratigraphy of Raisin 2. (a) Symbols and dates as in Figure 5. The coral base detached from the main slab is drawn in orange but was not X-rayed. Growth band counting on that part was based on growth rate of the species and growth band counting of the top (X-rayed) part. Blue rectangle: U/Th sample location with date and uncertainty (Table 1). (b) HLS curve of Raisin 2. Symbols, rates, and dates as in Figure 5. For the blue straight line, we have considered that the modern HLS outlined by new growths in 2008 is the last HLG (see Text S4 in the supporting information).

For Pointe Ecurie and Chancel islet, the mean submergence rates recorded since 1880 by the four sampled corals are in good agreement (about 2 mm/yr, Table 2). The mean submergence rates recorded by corals from Gros Raisins Bay are higher (between 3 mm/yr and 4 mm/yr, Table 2) but calculated over shorter periods (1914–2008 for Raisin 2 and 1947–2008 for Part 4 of Raisin 1, Table 2).

Plotting all HLS curves together (Figure 12a) illustrates that submergence rates are similar between samples during shared time periods. Furthermore, the majority of the die downs are correlated between records (Figure 12a). By plotting all HLS points together (Figure 12b), we infer a net submergence rate (based on the method of *Zachariasen* [1998], *Zachariasen et al.* [2000]) of 2.2 mm/yr since 1784 ± 15.

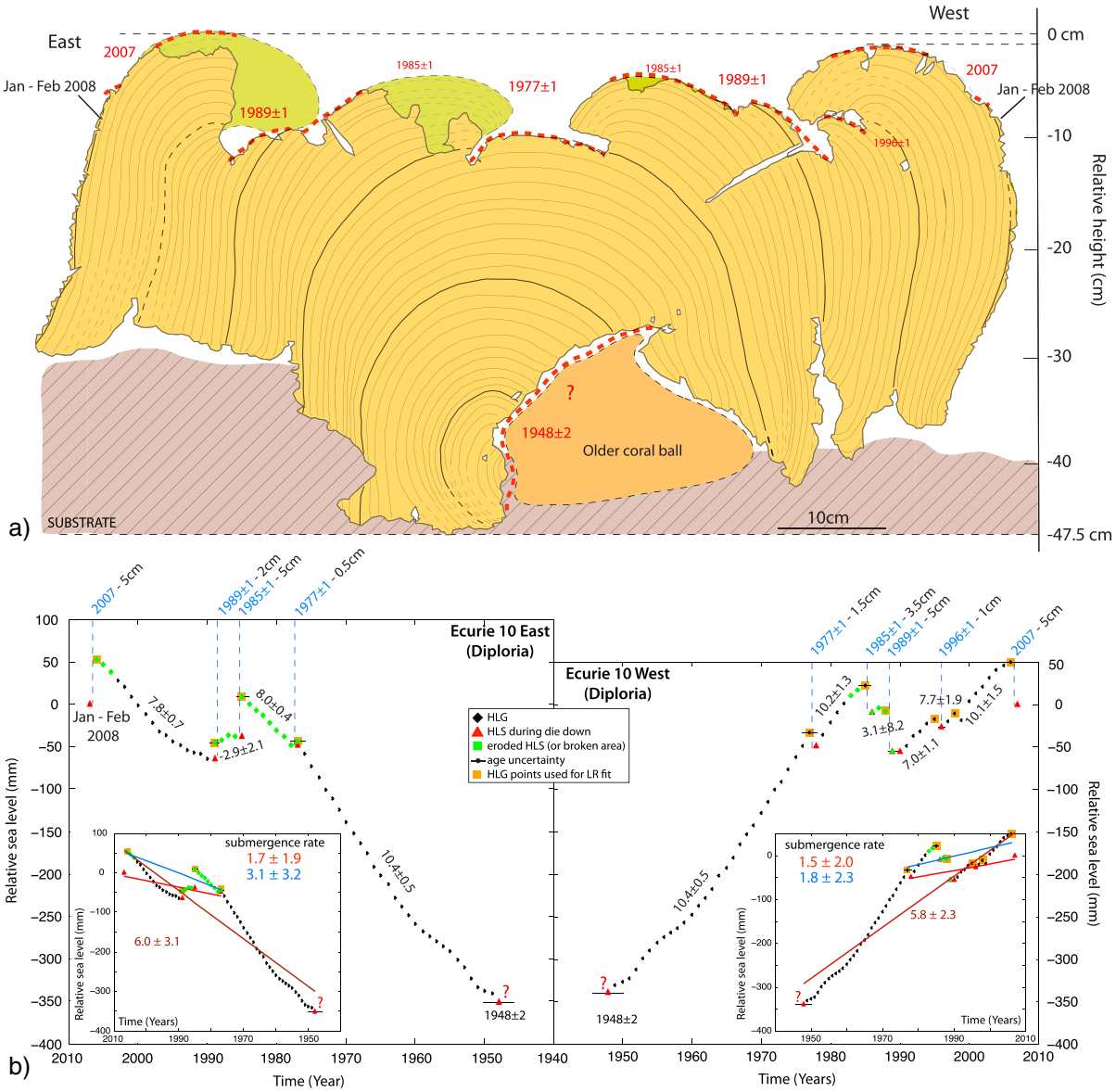

Figure 11. Slab stratigraphy of Ecurie 10.(a) Symbols and dates as in Figure 5. Green area: as in Figure 8a. The older coral on which Ecurie 10 began to grow is drawn in orange. (b) HLS curve of Ecurie 10. Symbols, rates, and dates as in Figure 5. The HLS curves have been constructed for each radius and positioned relative to each other. Inset: brown straight lines: submergence rate treating 1948 ± 2 as the first HLS (see Text S4 in the supporting information).

The geomorphology and stratigraphy of the coral microatolls clearly indicate changes in submergence rates through time: in 1829 ± 11 (rate changes between Parts 1 and 2 of Raisin 1 from 3.5 ± 1 mm/yr to about 1.0 mm/yr, Table 2), around 1895 (rate changes from 1.0 ± 0.4 mm/yr to 2.4 ± 0.7 mm/yr, mainly supported by Raisin 1 morphology with the transition from the very flat and partially eroded plateau of Part 2 to the more preserved coral surface of Part 3), and around 1950 with a rate increase from 2.4 ± 0.7 mm/yr to 3.3 ± 0.7 mm/yr (recorded in all corals as a decrease in the die down frequency following a die down around 1948 ± 1, and/or an abnormally long period of continuous upward growth) (Figure 12b).

An increase in submergence rate can be due to either a sudden or a gradual sea level increase, and we will discuss this in section 4.2.

3.5. Die Downs

The die downs recorded by corals from Martinique are sudden, with a maximal amplitude of 5 cm (variable between corals), and are followed by rapid upward growth at rates higher than submergence rates calculated over the whole HLS record. Die downs are not systematically recorded by all corals, some corals being slightly

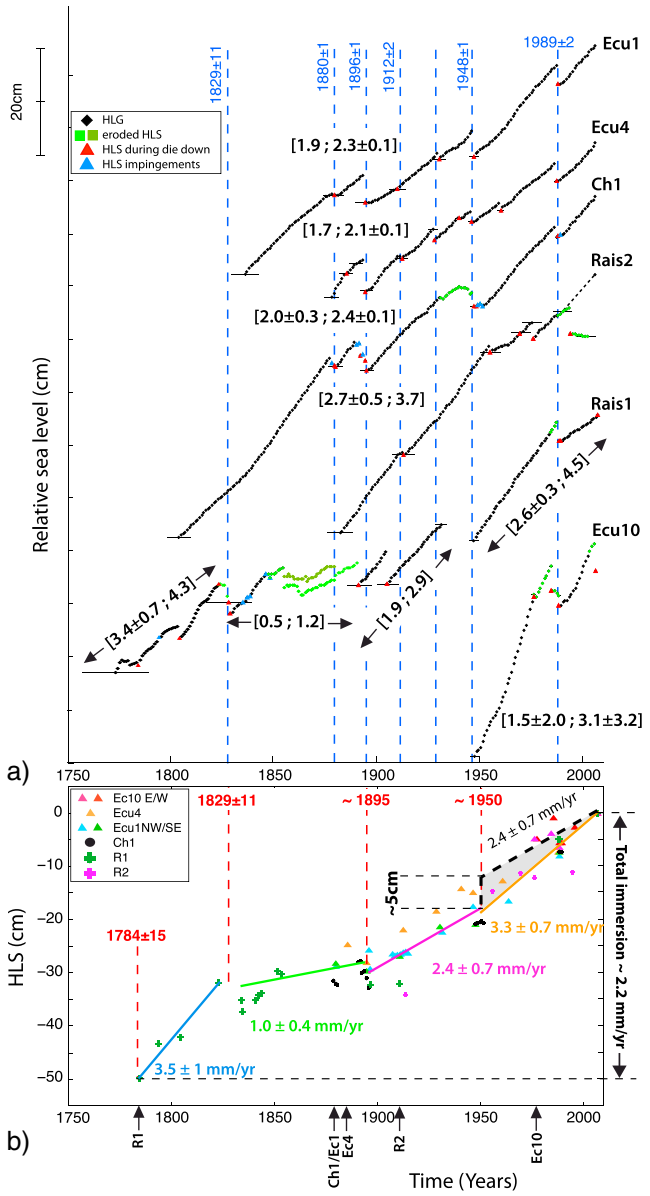

Figure 12. Combination of all HLS records. (a) HLS curves of each microatoll with their respective submergence rate ranges (calculated over their whole HLS record) in millimeters per year (Table 2). For Raisin 1, we separate the record with double arrows in four parts (see main text). Dashed blue lines: major die downs correlated between HLS records. (b) HLS points of all corals by taking into account their respective surveyed elevations. Blue, green, pink and orange lines: submergence rates calculated from 1784 ± 15 to 1829 ± 11, from 1829 ± 11 to 1895, from 1895 to 1950 and from 1950 to 2008, respectively. Dashed red lines: dates of major rate changes. Dashed black lines: magnitude of a sudden relative sea level rise inferred by assuming a constant submergence rate of 2.4 ± 0.7 mm/yr before and after 1950. Black arrows: beginning of HLS record of each coral.

deeper than others. The amplitude of die down does not vary with species. However, the die down frequency naturally varies with the coral growth rate of the species [*Zachariasen et al.*, 1999, 2000; *Natawidjaja et al.*, 2007]. The higher the growth rate, the more frequently die downs will be recorded.

Sometimes, all microatolls record the same die down, but with different amplitudes. For example, the 1989 ± 2 die down was recorded with larger amplitudes on Ecurie 1 and Ecurie 4 than on Chancel 1, though Chancel 1 was the shallower one. This suggests that the 1989 ± 2 die down and other die downs with similar characteristics are likely nontectonic events. A sea level drop due to tectonic uplift would rather have killed a larger

part of the top of shallower corals. Unusually low tides, occurring in the daytime, and lasting long enough to kill polyps are probably the cause of the die downs [e.g., *Taylor et al.*, 1987; *Zachariasen*, 1998]. Variability in amplitude of a die down likely reflects the sensitivity of the polyps to temporary emergence.

Die downs have also been documented in coral microatolls from the Indian and Pacific Oceans and were associated with climatic modes: El Niño–Southern Oscillation for the Pacific Ocean and the Indian Ocean Dipole for the Indian Ocean [e.g., *Woodroffe and McLean*, 1990; *Woodroffe and Gagan*, 2000; *Meltzner et al.*, 2010; *Philibosian et al.*, 2014]. In the Caribbean, the North Atlantic Oscillation (NAO), which is the dominant climatic mode at the interannual scale, may induce temporary sea level drops capable of causing coral die downs. Further investigation of the origin of the die downs is beyond the scope of this paper, because a study at a more regional scale would be required.

4. Causes of the Relative Sea Level Changes Recorded by the Microatolls

To interpret the signal recorded by our coral microatolls and distinguish between tectonic and climatic origin, we compare the HLS history we obtained to the regional sea level recorded by tide gauges. Toward this goal, we developed a Matlab code to model the growth of a coral by using a true tide gauge record. We first discuss the long-term sea level trend retrieved from several tide gauges in Florida and the northern Caribbean. We then use the tide gauge record of Key West, the longest and closest to Martinique, to model the growth of a synthetic coral microatoll in different relative sea level contexts.

4.1. Regional Sea Level Trend in the Tide Gauge Record

We selected 10 records [*Holgate et al.*, 2012], with more than 90% of completeness from Florida, the Gulf of Mexico, Puerto Rico, and Panama (locations in Figure 13), long enough (more than 50 years) to avoid bias in sea level trend due to interannual and interdecadal sea level variations [*Douglas and Peltier*, 2002; *Wöppelman and Marcos*, 2015]. We completed the data set with a 74 year composite relative sea level reconstruction assembled from shorter records localized closer to the Lesser Antilles (from the surrounding region of Hispaniola) [*Weil-Accardo et al.*, 2016]. Unfortunately, no continuous tide gauge record exists from Martinique or from other islands of the Lesser Antilles arc.

Submergence rates, estimated by linear regression, range between 1.4 ± 0.1 mm/yr (Cristobal; 1909–1981) and 9.0 ± 0.3 mm/yr (Grand Isle; 1947–2015) (Figures 13, S19, and Table 3). By excluding the two records of Galveston and Grand Isle that indicate submergence rates inconsistent with other tide gauges, probably due to local processes [e.g., *Penland and Ramsey*, 1990; *Blum and Roberts*, 2009], we calculate a mean regional submergence rate of 2.0 ± 0.8 mm/yr (Figure 13 and Table 3).

Most of the tide gauges are located in Florida and in the Gulf of Mexico. They record a significant signal related to the glacial isostatic adjustment (GIA) [*Clark et al.*, 1978]. Following the numerical predictions of *Tamisiea and Mitrovica* [2011], the GIA should range between 0.75 and 1 mm/yr in this area (Figure 13). It would, however, be negligible farther southward in the Lesser Antilles (0 to 0.15 mm/yr, i.e., within the uncertainties of the submergence rates inferred from corals, Figure 13).

The vertical land motion was recorded by GPS for five of the tide gauges we selected [*Wöppelmann et al.*, 2009; *Bouin and Wöppelmann*, 2010]. Those data are available at the Sonel website (http://www.sonel.org/) and can be used to correct the submergence rate determined from tide gauges for local or more regional tectonic signals such as the GIA (Table 3). The sea level rises at rates ranging between 0.9 ± 0.6 mm/yr (Galveston) and 1.7 ± 0.4 mm/yr (Key West) in the Gulf of Mexico and in Florida and by 0.7 ± 0.6 mm/yr (San Juan) in Puerto Rico, closer to Martinique (Table 3). These rates are lower than the submergence rates estimated without the GPS correction. The mean rate of sea level rise estimated from GPS-corrected tide gauges is 1.1 ± 0.8 mm/yr (Table 3). This value is in agreement with the post-1950 sea level reconstruction of *Palanisamy et al.* [2012], who calculate a mean rate of 1.8 ± 0.4 mm/yr of regional sea level rise over the 1950–2009 period and with the sea level rise of 1.7 ± 1.3 mm/yr inferred by *Torres and Tsimplis* [2013] for the Caribbean Sea for the period 1993–2010. This implies that a significant part of the long-term submergence recorded by coral microatolls in Martinique, where the GIA is low, cannot be accounted for by sea level rise and is likely due to local tectonics.

4.2. Coral Growth Modeling

We previously showed that the coral record suggests clear changes in sea level trend with slope breaks in 1829 ± 11, around 1895, and around 1950. The morphology of our corals also strongly differs from other

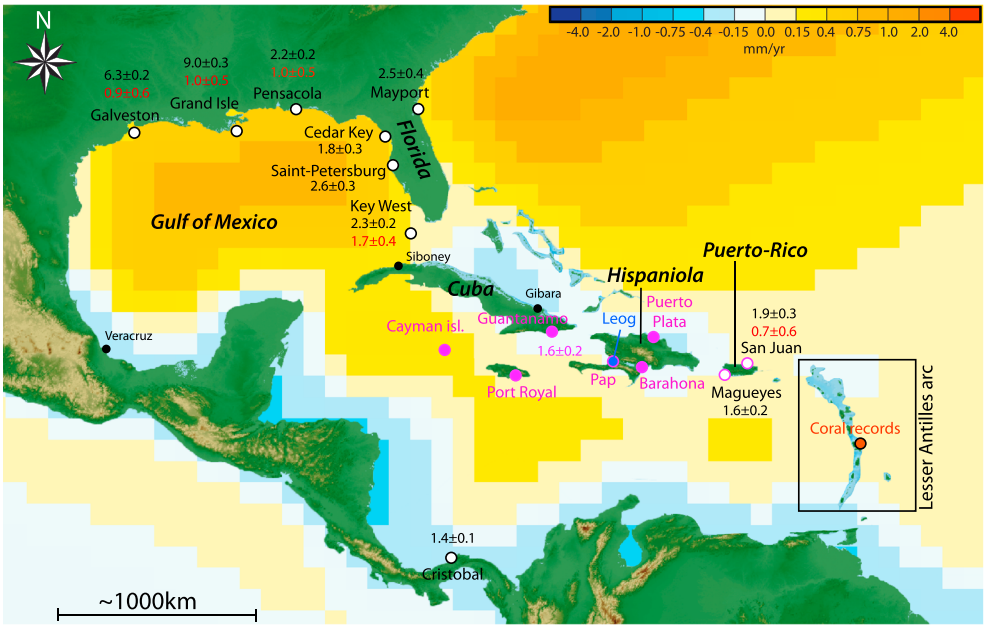

Figure 13. Map of regional tide gauge records. Topography: SRTM30+. Background with related color scale (top right corner): numerical prediction of the present-day impact of GIA on relative sea level measured by tide gauges [*Tamisiea and Mitrovica*, 2011]. White dots: tide gauge records of at least 50 years (PSMSL, http://www.psmsl.org/data/obtaining/). Pink dots: short-lived tide gauges used to construct a 74 year (1937–2011) composite monthly mean relative sea level record in Haiti [*Weil-Accardo et al.*, 2016]. Blue dot: location of coral microatolls from Léogâne (Leog) in Haiti [*Weil-Accardo et al.*, 2016]. Red dot: coral record from Martinique. Small black dots: additional tide gauges used in Figure S19. Black numbers: submergence rates calculated for each tide gauge (Table 3). Red numbers: rate of sea level rise from GPS-corrected tide gauges (SONEL, http://www.sonel.org/) (Table 3). Pink number: submergence rate inferred from the composite relative sea level curve in Haiti [*Weil-Accardo et al.*, 2016] (Table 3). Black rectangle: Lesser Antilles arc.

Table 3. Regional Sea Level Rise (in Millimeters Per Year With 2σ Uncertainty)[a]

Tide Gauge (Time Span)	Submergence Rate	GPS Signal	Sea Level Rise
Galveston (1908–2015)	6.3 ± 0.2	-5.4 ± 0.6	0.9 ± 0.6
Grand Isle (1947–2015)	9.0 ± 0.3	-8.0 ± 0.2	1.0 ± 0.5
Pensacola (1923–2015)	2.2 ± 0.2	-1.2 ± 0.4	1.0 ± 0.5
Mayport (1928–2000)	2.5 ± 0.4	-	-
Cedar Key (1939–2015)	1.8 ± 0.3	-	-
Saint-Petersburg (1947–2015)	2.6 ± 0.3	-	-
Key West (1913–2015)	2.3 ± 0.2	-0.6 ± 0.4	1.7 ± 0.4
Haiti composite curve (1937–2011)	1.6 ± 0.2	-	-
San Juan (1962–2015)	1.9 ± 0.3	-1.2 ± 0.5	0.7 ± 0.6
Magueyes (1955–2015)	1.6 ± 0.2	-	-
Cristobal (1909–1981)	1.4 ± 0.1	-	-
Regional submergence	2.0 ± 0.8[b]	-	-
Regional sea level rise	-	-	1.1 ± 0.8

[a]Submergence rate calculated by linear regression (Figure S19) for each tide gauge in Figure 13 (PSMSL, http://www.psmsl.org/data/obtaining/) and for the composite curve produced from several tide gauges surrounding Haiti [*Weil-Accardo et al.*, 2016]. With available GPS records (SONEL, http://www.sonel.org/), we estimate the rate of sea level rise recorded by tide gauges.

[b]We do not take into account the record of Galveston and Grand Isle, which are excessively influenced by local processes, making them inconsistent with other records.

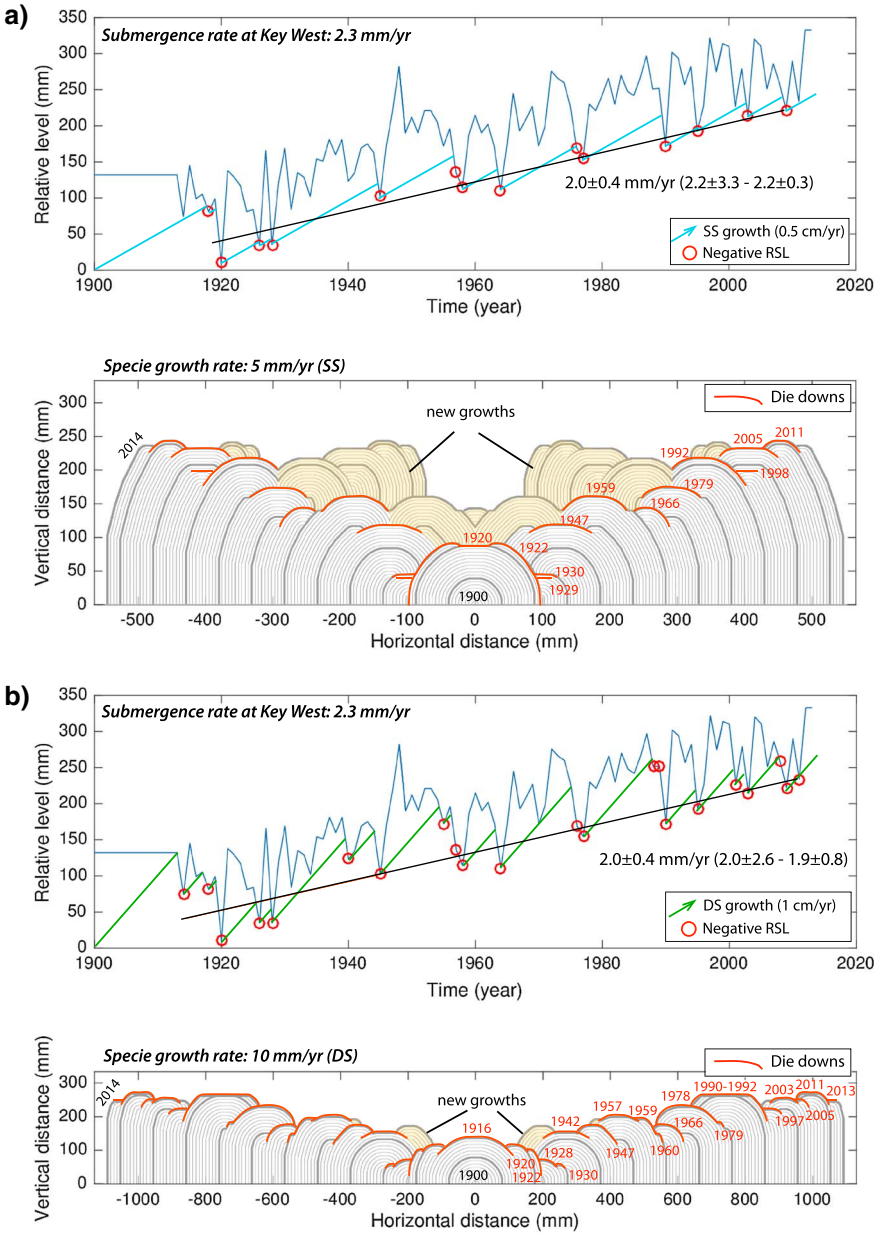

Figure 14. Modeling of microatoll growth at Key West. Modeling of the growth of a (a) *Siderastrea siderea* (SS) coral and a (b) *Diploria strigosa* (DS) coral, based on the 100 year Key West tide gauge record (annual minima). Blue and green lines: hypothetical coral microatoll growth. Black straight lines: submergence rates (with 2σ uncertainties) calculated by linear regression (LR) with only HLS points [*Zachariasen*, 1998; *Zachariasen et al.*, 2000]. Black numbers in brackets: submergence rates calculated with HLS points before and after 1950.

microatolls we sampled in Haiti. The latter corals are rather flat or slightly cup-shaped and record submergence at constant rate of ≈1 mm/yr over the last century [*Weil-Accardo et al.*, 2016], whereas the Martinique corals display pronounced cup shapes (indicating more rapid submergence), columnar growths, or plateaus. The difference in shape of microatolls sampled only a few hundred kilometers apart in the Caribbean basin supports a local tectonics signal in Martinique since the climatic signal (sea level rise, interannual and decadal anomalies) should be uniform at that scale.

As the tide gauge records we used began only in 1908, they are too short to have documented the first two changes in submergence rate recorded by corals from Martinique. However, they could be useful to document the relative sea level change that occurred around 1950. In every tide gauge record, it is very difficult,

due to large interannual and interdecadal anomalies, to discern a clear change in submergence rate at that time. Although coral microatolls act as natural tide gauges and record the same sea level trends (as well as smaller timescale anomalies) as a true tide gauge, the two signals cannot be easily compared. To overcome this problem, we developed a Matlab code to model the growth of a microatoll by using a true tide gauge record. To reduce computing time and because die downs typically occur at the annual lowest sea levels, we extracted an annual record from the monthly tide gauge record by considering only the lowest sea level value of each year. We used the Key West tide gauge, which is the longest record from Florida, and also the closest to the Lesser Antilles arc. This tide gauge records relative sea level changes at different timescales since 1913, including interannual temporary positive and negative sea level anomalies that may control the coral development and morphology. We compared the Key West record to other tide gauge records in the Caribbean (Figure S19). The record of Key West is representative of the regional signal, since we identified synchronous sea level anomalies in other regional tide gauges (Figure S19). Although no tide gauge record over more than 10 years exists in the Lesser Antilles, it appears reasonable to assume that the interannual signal would be similar to that of Key West (and other regional tide gauges), as climatic phenomena that drive sea level anomalies likely occur at the scale of the whole Caribbean area.

We produced two synthetic corals (as they would have developed at Key West): a *Siderastrea siderea* (SS) (growth rate of 5 mm/yr) and a *Diploria strigosa* (DS) (growth rate of 10 mm/yr) microatoll (Figure 14). They both have a regular cup morphology indicating a relative sea level increase at a constant rate (2.0 ± 0.4 mm/yr, Figure 14) in agreement with the submergence rate of 2.3 mm/yr recorded at Key West. Since the DS is growing twice as fast as the SS, it is killed twice as often by low sea level anomalies than the SS. Consequently, about 20 die downs are recorded by the DS in about one century whereas only 10 are recorded by the SS (Figure 14). Linear regression across the synthetic HLS points shows that the submergence rate is constant over one century with no acceleration around 1950 (Figure 14). This contrasts with the Martinique corals.

Additionally, in these simulations, die downs occur regularly, every $\approx 6 \pm 4$ years for the DS and every $\approx 13 \pm 4$ years for the SS. This frequency was not observed in most of our *Siderastrea siderea* specimens, which exhibit a lack of die downs over a long period between 1947 ± 2 and 1989 ± 1 (42 years). A constant sea level rise, as recorded in a tectonically stable area in Florida, cannot account for the morphology of the microatolls we sampled in Martinique. This difference clearly indicates that local tectonics are at work.

To determine the origin of and quantify the local tectonic processes (increase in submergence rate or sudden submergence), we attempt to reproduce the shape of our microatolls by using information from their HLS history. We focused on the Ecurie 1 and Chancel 1 microatolls because they both have long records, reached their HLS during the die down of 1948 ± 2 (contrary to Raisin 1, Raisin 2, and Ecurie 10 which were below their HLS around 1950; Figure S20 and Text S5 in the supporting information), and have much simpler shapes that we expect to be easier to reproduce.

We first remove the relative sea level trend recorded at Key West and further artificially apply either (1) submergence rates of 1.4 mm/yr between 1913 and 1950 and 3.5 mm/yr between 1950 and 2015 as determined from the Ecurie 1 and Chancel 1 records (Figures 15b–15d) or (2) a sudden sea level increase of ≈ 12 cm between two periods of constant sea level rise at 1.4 mm/yr (according to the record of Ecurie 1; Figures 15b and 15e). Through these simulations, we show that an increase of 2.1 mm/yr in the rate of submergence did not induce a major morphological change in the coral stratigraphy and in the die down frequency (one die down every ≈ 10–15 years between 1913 and 1950 and one die down every $\approx 13 \pm 5$ years between 1950 and 2015) (Figure 15d), whereas a sudden sea level increase by a few centimeters was sufficient to drown the coral and to preserve it from further sea level drops for the following 32 years (Figure 15e). Although the model is simplified by the use of a constant growth rate of 5 mm/yr, these results suggest that our microatolls were drowned by a few centimeters during a sudden tectonic event.

This hypothesis is also compatible with the record of the *Diploria strigosa* microatoll Ecurie 10. This microatoll recorded five die downs between 1977 and 2008 (implying that this period experienced sea level drops similar in frequency and amplitude to the ones recorded by *Siderastrea siderea* corals between 1880 and 1950) and a rate of relative sea level increase of ≈ 1.5–2 mm/yr between 1977 ± 1 and 2008 (Figure 11b). This rate is similar to the submergence rate recorded by Ecurie 1, Ecurie 4, and Chancel 1 before 1950 (between 1.4 ± 0.7 mm/yr and 2.1 ± 0.7 mm/yr; Figure S21 and Text S5 in the supporting information). The history of Ecurie 10 thus supports that the corals experienced a sudden relative sea level increase around 1950 rather than an increase in submergence rate.

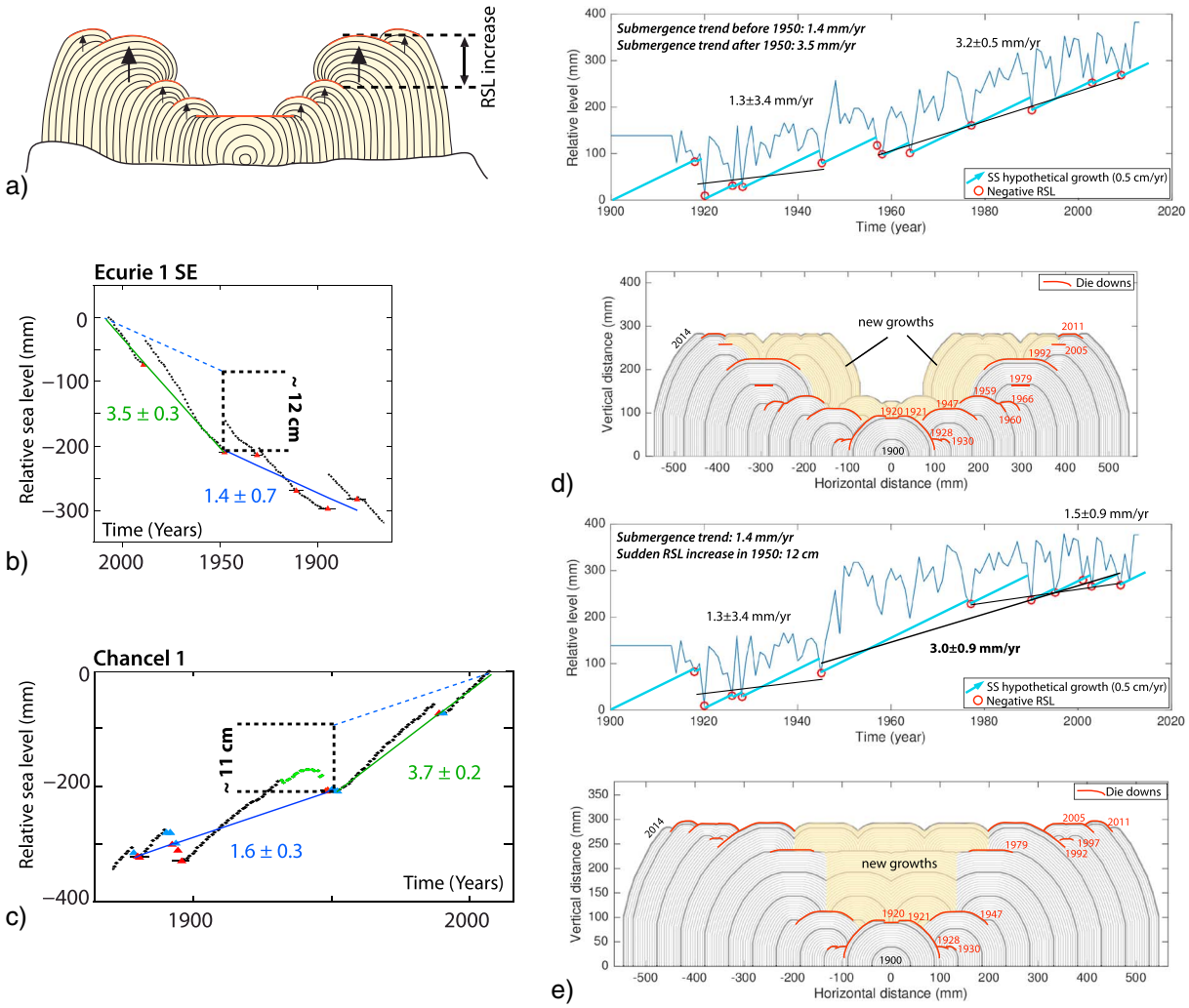

Figure 15. Modeling of the morphological changes recorded by corals around 1950. (a) Schematic drawing of the changes recorded around 1950 (see text). (b, c) HLS curves of Ecurie 1 and Chancel 1. Blue and green lines: submergence rates (in mm/yr) before 1950 and after 1950, respectively. Dashed black lines: estimate of the sudden increase around 1950. Modeling of a SS coral microatoll growth based on Key West tide gauge with the long-term trend removed. (d) Submergence trend increase in 1950 from 1.4 mm/yr to 3.5 mm/yr and (e) steady submergence rate (1.4 mm/yr) with a sudden relative sea level increase of 12 cm in 1950. Black straight lines: as in Figure 14. In Figure 15e we also calculate the submergence rate between the 1947 die down and 2015.

Before 1900, according to *Kemp et al.* [2009, 2011], at the global scale, the sea level was relatively stable or slightly decreasing during the Little Ice Age, before beginning to increase at 2.1 mm/yr around A.D. 1865–1892. This transition around A.D. 1865–1892 may explain the submergence increase recorded by corals around 1895 (Figure 12b). However, the submergence rates of 3.5 ± 1 mm/yr (recorded by Raisin 1) between 1784 ± 15 and 1829 ± 11 and of 1.0 ± 0.4 mm/yr (recorded by Raisin 1 and Chancel 1) between 1829 ± 11 and 1895 (Figure 12b) are not compatible with the results of *Kemp et al.* [2009, 2011].

5. Origin of Tectonic Deformation

Since the regional sea level signal cannot explain the whole coral record, an additional process that could generate land subsidence (on the order of a millimeter per year with rate fluctuations through time) is needed to explain the HLS record.

5.1. Volcanoes and Shallow Crustal Faults

As Martinique is an active volcanic island surrounded by numerous active crustal faults, we have to consider both volcanic and fault processes as possible sources of vertical movement.

Volcanic processes are associated with land deformation. While magmatic chamber inflation may lead to long-term uplift of the volcano and surroundings, voiding of the magmatic chamber during eruptions may induce significant land subsidence [e.g., *Mogi*, 1958; *Newman et al.*, 2012]. Such ground motions could be recorded by coral microatolls. Robert and Galion Bays are about 30 km away from the Mount Pelée edifice. We have calculated that for a magmatic chamber lying at 5 km depth [*Feuillet et al.*, 2011a], a volume variation larger than 0.16 km^3 (typical of large eruptions of Soufriere Hills volcano in Montserrat, e.g., *Young et al.* [1998], *Sparks et al.* [1998]) would be needed to generate subsidence of a few centimeters in Robert and Galion Bays. During the last two centuries, Mount Pelée volcano erupted two times: between 1902 and 1905 and between 1929 and 1932 [e.g., *Boudon*, 2011]. No submergence rate change in the coral record corresponds to these two eruptions. We have calculated that filling the magmatic chamber (constant refilling rate in a spherical chamber in an elastic half space with $\mu = 32$ GPa) would produce an uplift rate on the order of one tenth of a millimeter per year, which is clearly too low to be recorded by the Martinique corals.

Numerous active faults with metric to decametric offsets have been identified around Martinique Island [*Savry*, 2007; *Feuillet et al.*, 2011a]. They mainly crosscut the island in a NNW-SSE direction and extend offshore in the channels between islands, south of the St-Anne Peninsula and north of Mount Pelée (Figure 1b) [*Feuillet et al.*, 2011a]. These faults may move at rates of a few tenths of a millimeter per year, comparable to slip rates determined for similar crustal faults on Guadeloupe [*Feuillet et al.*, 2004, 2011b], and have impacts limited within a radius similar to the fault depth (at most tens of kilometers). These faults are clearly too far from Galion and Robert Bays to induce ground motions as large as those recorded by our corals.

5.2. The Megathrust Seismic Cycle

Rather than local tectonics, it is likely that the microatolls of Martinique, which lie above the Lesser Antilles megathrust, have recorded vertical land motion related to the seismic cycle of the megathrust as documented in Sumatra [e.g., *Sieh et al.*, 2008].

Two $M > 7$ earthquakes may have ruptured the megathrust on 11 January 1839 and on 21 May 1946 and causing significant deformation in the upper plate. During the interseismic period, the strain accumulation along the plate interface may have induced long-term deformation at a rate of several millimeters per year, fast enough to control coral growth.

5.2.1. The 11 January 1839 Earthquake

Two microatolls we sampled (Raisin 1 and Chancel 1) were growing during the major historical earthquake of 11 January 1839, of magnitude ≈8 [*Robson*, 1964; *Feuillard*, 1985; *Feuillet et al.*, 2011a].

This earthquake is the largest known event reported in Martinique, with significant damage and the destruction of Fort-de-France (previously Fort-Royal). The macroseismic intensities imply an epicenter location offshore Martinique. While *Feuillard* [1985] suggests an intensity of 8 in Martinique, *Robson* [1964] favors a higher intensity of 9 for the island. The initial magnitude of 7.5 estimated by *Feuillard* [1985] has been recently reassessed to 8 by using the B^3 attenuation law [*Beauducel et al.*, 2011]. This earthquake, which is likely a megathrust event, broke a 140 km long segment [*Feuillet et al.*, 2011a].

The major change in morphology of Raisin 1 in 1829 ± 11 corresponds well to the 1839 earthquake. We have shown that the oldest part of the coral may have been tilted, perhaps transported into shallower water, and buried by sand (see the Raisin 1 description in section 3.3.2), making it impossible to use this coral to calculate a coseismic displacement for the 1839 event. Tsunamis or hurricanes can break, move, and overturn microatolls. We verified that no major hurricane struck Martinique at that time (Table 4). Our coral may have been reworked by a small tsunami (as no significant tsunami has been reported in association with the 1839 earthquake in historical records).

The major submergence rate decrease (from about 3.5 ± 1 mm/yr to about 1 mm/yr) recorded by Raisin 1 around 1829 ± 11 is striking. It correlates with the occurrence of the 1839 earthquake and persisted over several decades (50–60 years) after the event. Such fluctuations in vertical deformation rate (as changes in rate of relative sea level) after an earthquake have been observed in numerous microatolls at several sites in Sumatra or Vanuatu. For example, this was documented in Sumatra after the megathrust earthquakes of 1600 [*Sieh et al.*, 2008] and 1797 [*Philibosian et al.*, 2014]. These rate changes have been interpreted as the result of (1) changes in the degree of interseismic coupling on the megathrust interface (an usually strongly coupled patch, able to promote large earthquakes, may become transiently weakly coupled after a large earthquake) [*Philibosian et al.*, 2014], (2) variations in locking depth, or (3) changes in fluid conditions

Table 4. Major Hurricanes in the Lesser Antilles Since[a]

Date[b]	Hurricane Name	Category	Affected area	Damages
1780	—	5	from BARB to G.A	> 20,000 deaths in the Caribbean
≈1787	—	—	FA	—
≈1805	—	—	FA	—
7/26/1825	—	—	GUAD	300 deaths (BT, MG)
9/6/1865	—	—	GUAD	80 deaths (MG)
≈1875	—	—	FA	—
8/18/1891	—	—	MART	700 deaths in MART
9/12/1928	—	4	GUAD	> 1200 deaths in Pointe-à-Pitre
8/21/1950	BAKER	1	GUAD, ANT	—
9/1/1950	DOG	2-3	ANT-BAR, STBART	—
8/11/1956	BETSY	1-2	DOM, GUAD	numerous tens of deaths
9/4/1960	DONNA	4-5	STMART, ANG	numerous tens of deaths
9/25/1963	EDITH	2 to 3-4[c]	MART	>10 deaths
10/1/1963	FLORA	1	BARB, GREN	minor destructions in the south part of the arc
8/22/1964	CLEO	3	GUAD	14 deaths and important destructions
9/27/1966	INEZ	4	GUAD, DOM, ANT	25 deaths
8/29/1979	*DAVID*	4-5	DOM, MART, GUAD	> 50 deaths in DOM
9/16/1989	*HUGO*	4-5	GUAD to Virgin islands	> 100 deaths in the Caribbean
9/4/1995	LUIS	4	from GUAD to ANG	larger destructions in ANT-BARB
9/15/1995	MARYLIN	1	GUAD, MART, ANT	no major destructions along the arc
9/20/1998	GEORGES	3-4	GUAD, ANT-BAR, STKIT-NEV	important destructions in STKIT-NEV
11/19/1999	LENNY	TP[d]	GUAD	west wind on the lee shore
2004	IVAN	2-3	STLU to GREN	39 deaths in the Caribbean to GREN
8/16/2007	DEAN	2	MART, STLU	important destructions in MART
10/16/2008	OMAR	3	STMART, STBART	west wind on the lee shore

[a]Sources: http://www.meteo.fr/temps/domtom/antilles/pack-public/cyclone/, http://www.emdat.be/, [*Zahibo et al.*, 2008, 2008; *Meteorological Service of the Netherlands Antilles and Aruba*, 2010; *Garnier et al.*, 2015]. Abbreviations: GUAD: Guadeloupe, BT: Basse-Terre (GUAD), MG: Marie-Galante (GUAD), MART: Martinique, ANG: Anguilla, STLU: Sainte-Lucia, DOM: Dominica, ANT-BAR: Antigua and Barbuda, STMART: Saint-Martin, STBART: Saint-Barthélémy, STEU: Saint-Eustache, BARB: Barbados, STKIT-NEV: Saint Kitts and Nevis, GREN: Grenada, G.A: Greater Antilles. Major hurricanes HUGO and DAVID (written in italics) significantly affected the French Antilles (FA).

[b]Dates are formatted as month/day/year.

[c]The category of EDITH hurricane varies with reference sources.

[d]LENNY reached the category 3–4 around the north islands of the arc before declining to a tropical storm (TP) around Guadeloupe.

[*Meltzner et al.*, 2012, 2015]. Such interseismic strain rate switching may occur from one earthquake cycle to the next or within a single earthquake cycle and could be a common phenomenon in subduction zones [*Meltzner et al.*, 2012, 2015; *Philibosian et al.*, 2014]. This implies that megathrust faults might have a behavior more complex than simple elastic strain accumulation and relief [*Meltzner et al.*, 2010, 2015].

Chancel 1 was also growing when the earthquake occurred. This coral grew freely between 1805 ± 6 and 1881 ± 4 (before its first HLS impingement) over a period of about 75 years, which is much longer than the hemispherical growth period observed (up to 40 years) for other microatolls of the same species. Chancel 1 seems to have grown in deeper water. Such a long-lasting period of growth may be accounted for by a sudden submergence. This could indicate coseismic subsidence during the 1839 earthquake.

5.2.2. The 21 May 1946 Earthquake

The most damaging earthquake of the twentieth century in Martinique occurred on 21 May 1946, close to the Caravelle Peninsula, 50 km off the eastern coast of Martinique and at a depth between 50 km and 60 km [*Dorel*, 1981; *Feuillard*, 1985; *Russo et al.*, 1992]. It was felt from the island of Saint-Vincent to the Guadeloupe archipelago [*Robson*, 1964; *Feuillard*, 1985]. The shaking intensity peaked on Martinique, reaching 8 [*Feuillard*,

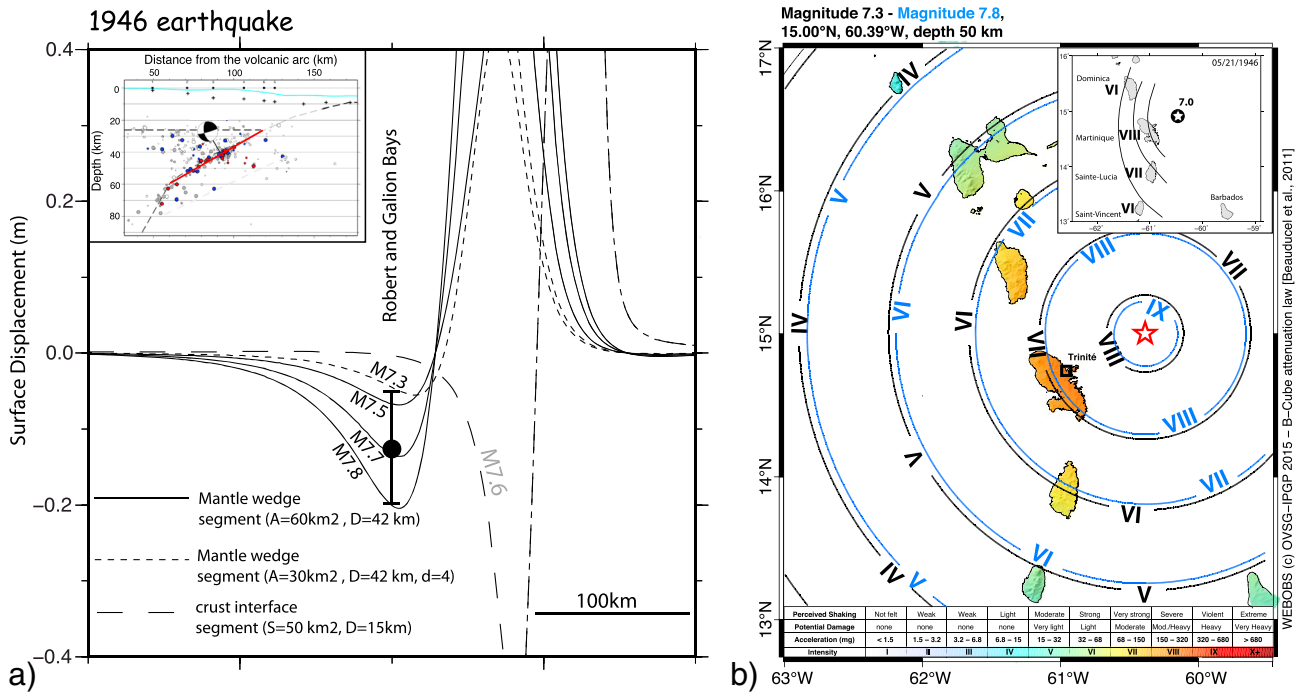

Figure 16. (a) Elastic dislocation modeling [*Okada*, 1992] of the coseismic vertical deformation related to the 21 May 1946 earthquake. Inset: Thrust geometry outlined by seismicity [*Laigle et al.*, 2013; *Ruiz et al.*, 2013]. Red line: segment which may have broken on 21 May 1946. Black dot with uncertainty: subsidence inferred from coral microatolls, ranging between 5 cm and 20 cm. (b) Simulations using a local macroseismic intensity prediction equation [*Beauducel et al.*, 2011] for an earthquake of magnitude of 7.3 (in black) and 7.8 (in blue) with an epicentral location of 15°N, 60.39°W and a depth of 50 km. The calibrated color scale corresponds to the simulation for an earthquake of magnitude of 7.8. Inset: Isoseismal map for the 21 May 1946 earthquake from *Dorel* [1981].

1985], and considerable destruction was documented there [*Feuillard*, 1985]. The date of this earthquake correlates strikingly with the change in microatoll morphology around 1950, which we have inferred to be due to a sudden subsidence event.

The magnitude of this sudden subsidence event, probably of coseismic origin, can be grossly estimated. By using coral growth modeling, we previously inferred that this change can be accounted for by a sudden submergence of a few centimeters around 1950. By considering all HLS points (Figure 12b), and assuming a constant submergence rate of 2.4 ± 0.7 mm/yr since 1895 before and after 1950, the tectonic subsidence can be estimated to be 5 cm (Figure 12b). By analyzing the various individual HLS records, we estimate that tectonic subsidence ranged between a few centimeters and 20 cm (Figures S20, S21, and Text S5 in supporting information).

5.3. Elastic Dislocation Forward Modeling

We performed simple, conventional and widely used elastic dislocation models [*Okada*, 1992; *Savage*, 1983; *Kanda and Simons*, 2010] to test (1) whether the 1946 earthquake could have produced centimetric subsidence in Galion and Robert Bays given the source parameters available in the literature; and (2) whether the long term submergence recorded by our corals could be produced by interseismic strain accumulation along the megathrust.

5.3.1. The 1946 Earthquake

The geometry of the trench beneath Martinique is well known thanks to recent seismological investigations [e.g., *Laigle et al.*, 2013] (Figure 16 a, inset). Three-dimensional relocation of numerous earthquakes, including a $M > 5$ event in 2006, recorded by ocean bottom seismometers (OBS) offshore of the Caravelle peninsula, revealed clear seismic activity at the interface between the subducting American plate and the mantle wedge at depths between 30 km and 80 km [e.g., *Laigle et al.*, 2013]. This seismicity clearly outlines the geometry of the interface with a dip increasing westward from 30° to 57°, forming a kink at 60 km depth, 50 km from the subduction deformation front. The less steep segment is 60 km wide along the dip. The hypocenter of

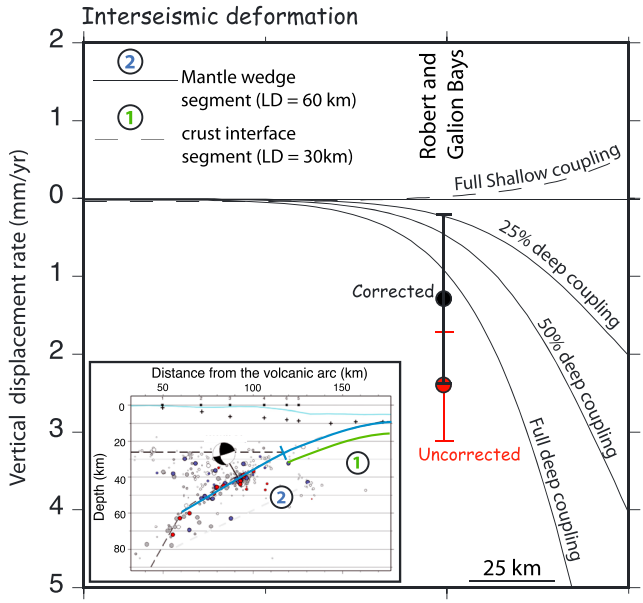

Figure 17. Elastic dislocation modeling of the interseismic deformation rates at the surface above the megathrust interface [*Savage*, 1983; *Kanda and Simons*, 2010] for different segments of the megathrust (drawn in green (1) and blue (2) in the inset). LD: locking depth. Black dot: corrected submergence rate attributed to interseismic deformation, if 1.1 ± 0.8 mm/yr of the submergence recorded by coral microatolls of Martinique since 1895 is due to the regional sea level rise. Red dot: uncorrected submergence rate if the entire submergence recorded by coral microatolls since 1895 is related to interseismic deformation. Inset: as in Figure 16a.

the 1946 earthquake was located by *Russo et al.* [1992] at 50 km depth, close to Martinique, in this area of deep seismicity. The earthquake is characterized by a thrust-faulting mechanism with a nodal plane dipping 20° westward, similar to the dip of the subduction interface at that location. The strike of this nodal plane is parallel to the subduction front. This earthquake probably ruptured the portion of the interface between the oceanic crust and the mantle wedge at depths between 30 km and 60 km. The magnitude of this earthquake is not well constrained, ranging between M_s 6 [*Russo et al.*, 1992] and 7 [*Gutenberg and Richter*, 1954].

We calculate the vertical displacement induced in an elastic half space with $\lambda = \mu = 32$ GPa, by a 60 km^2 (or 30 km^2) dislocation, dipping 30°W and striking 156°N, centered at 60.39°W, 15°N, and 42 km depth, with various amounts of slip (Figure 16a). Slip on such a dislocation generates centimeter scale subsidence in Robert and Galion Bays where our microatolls were growing (Figure 16a). Five to 20 cm of sudden subsidence requires uniform slip ranging between 2 and 6 m. The corresponding magnitude would range between 7.3 and 7.8 [*Kanamori*, 1977; *Wells and Coppersmith*, 1994] (Figure 16a), which is higher than that estimated for this event. However, by using the new B^3 attenuation law [*Beauducel et al.*, 2011], we verified that such magnitudes are compatible with the reported macroseismic intensities of *Dorel* [1981] (Figure 16b). As the B^3 model can predict macroseismic intensities within ±1.4 (1σ) on the MSK scale [*Beauducel et al.*, 2011], it will be essential to analyze the instrumental record of the 1946 earthquake preserved in the Seismic Research Centre of the University of the West Indies (SRC-UWI) in Trinidad and Tobago [*Russo et al.*, 1992], to better characterize the earthquake magnitude. This is beyond the scope of this work and deserves future investigation. With uniform slip, our dislocation model is oversimplified and cannot be used to determine the magnitude precisely. However, the modeling results are in agreement with subsidence of a few centimeters along the eastern coast of Martinique above the edge in front of the seismic rupture.

5.3.2. Deep Interseismic Loading

We have shown that our corals recorded long-term submergence at a mean rate of 2.4 ± 0.7 mm/yr since 1895. A part of this submergence is due to the regional sea level rise (1.1 ± 0.8 mm/yr since ca. 1900). As the long-term submergence recorded by corals is somewhat higher than the regional sea level rise (although the uncertainties do overlap), this means that corals might have recorded a residual tectonic submergence of a few tenths of a millimeter per year.

Following the procedure described by *Kanda and Simons* [2010] for curved faults, we first modeled the deformation induced by interseismic loading of the deeper segment (mantle wedge) by applying backslip [*Savage*, 1983] on a 57°W dipping dislocation with a locking depth at 60 km (Figure 17). We then calculate the interseismic deformation induced by loading of the crust-crust interface, with backslip on a dislocation dipping 30°W and locked at 30 km depth (Figure 17). We vary the percentage of coupling between 0.25 and 1. Full coupling of the shallowest segment induced very little uplift (less than 0.1 mm/yr) at the location of Robert and Galion Bays, whereas coupling ranging between 0.25 and 1 of the deeper mantle wedge segment produces 0.2 to 1 mm/yr of subsidence at these sites (Figure 17). It is clear that we do not have enough data and the uncertainties in the regional sea level rise are too large to make a firm conclusion about the coupling of the megathrust. However, this preliminary modeling shows that interseismic loading at depths ranging between 30 km and 60 km in the mantle wedge, in the area of sustained seismic activity [*Laigle et al.*, 2013; *Ruiz et al.*, 2013], is the only way to explain significant subsidence in Robert and Galion Bays.

If related to interseismic strain accumulation, the coral subsidence implies a significant degree of coupling of a megathrust. This contrasts with the results of *Manaker et al.* [2008] and *Symithe et al.* [2015] that indicate little or no coupling along the Lesser Antilles megathrust between Puerto Rico and Trinidad on the basis of GPS data. As GPS and coral records are of very different duration (a few years for the GPS, several decades for the corals), such a discrepancy between geodetic data and the Martinique coral record may be accounted for by a decrease in interseismic strain rate over the last several years. This might be related to interseismic strain rate switching, as previously described. However, the GPS data are very short term, sparsely distributed in a complex plate tectonic framework, far from the deformation front, and have poorly resolved vertical components. As such, they may not be as reliable as corals to quantify the long-term coupling rate along the megathrust.

6. Conclusion

We have presented the first study of coral microatolls in the Lesser Antilles arc. We use them to reconstruct relative sea level changes since the end of the eighteenth century in Robert and Galion Bays, on the east side of Martinique. The coral record consists of an interannual signal, with sudden oceanographic die downs that could be caused by climatic modes (mainly the NAO, which is the dominant climatic mode in the Caribbean at the interannual scale). A long-term submergence signal, estimated at 2.4 ± 0.7 mm/yr since around 1895, is superimposed on the interannual record. Before 1895, submergence rates inferred from coral microatolls fluctuate through time, with rates lower or higher than 2.4 ± 0.7 mm/yr. To explain the long-term submergence inferred from corals, we characterized the regional sea level trend with tide gauges and GPS records [*Wöppelmann et al.*, 2009]. As no definite acceleration is apparent in tide gauge records, we assume that the changes in submergence rates through time cannot be explained by the regional sea level rise [*Palanisamy et al.*, 2012; *Meyssignac et al.*, 2012], estimated to be 1.1 ± 0.8 mm/yr since the beginning of the twentieth century. We estimate that about 1.3 ± 1.1 mm/yr of submergence must be related to a nonclimatic process. Active crustal faults crossing and/or surrounding Martinique Island and volcanic activity of Mount Pelée generate signals too small to explain the microatoll data. Such vertical deformation rates are within the uncertainties of the submergence rates inferred from corals. Moreover, we did not find any correlation between the Mount Pelée eruptions of 1902–1905 and 1929–1932 and the coral record. A regional process generating subsidence in eastern Martinique is required. The Lesser Antilles megathrust is the most likely tectonic structure for generating such vertical deformation. Through a detailed analysis of the coral stratigraphy, we inferred a decrease in the die down frequency for Ecurie 1, Ecurie 4, and Chancel 1 corals, associated to a columnar upward growth around 1950. At the same time, the three other microatolls (Ecurie 10, Raisin 1, and Raisin 2) recorded an unusually long period of uninterrupted upward growth. With the development of a Matlab code to model coral microatoll growth, we demonstrated that this 1950 change in growth style is probably due to a sudden increase in the relative sea level of up to 20 cm. The persistence of the submergence suggests a tectonic source. The 21 May 1946 *M*7 earthquake [e.g., *Russo et al.*, 1992, and references therein] is the best candidate to explain our observations. With a simple elastic dislocation model, we have shown that the magnitude of the event would range between 7.3 and 7.8 in order to generate 5 cm to 20 cm of subsidence in Robert and Galion Bays. This magnitude would be in agreement with macroseismic intensities when modeled with the new B^3 attenuation law [*Beauducel et al.*, 2011]. Further analysis of instrumental data will be needed in order to reassess the event magnitude. New insights into the deep structure of the megathrust

[*Laigle et al.*, 2013; *Ruiz et al.*, 2013] have allowed us to deduce that the 1946 earthquake and likely the *M*8 1839 historical earthquake likely ruptured the deep section of the seismogenic interface, at the slab-forearc mantle interface. In that case, the 1839 earthquake would also have generated subsidence in eastern Martinique. Although we need more data to characterize the coseismic vertical motion associated with the 1839 earthquake and the possibility of a tsunami, the longest coral record (Raisin 1) exhibits a major submergence rate decrease after the earthquake. This could be interpreted as a coupling change on the subduction interface through the megathrust seismic cycle (triggered by a megathrust rupture). Finally, as the coral signal seems to be impacted by subduction earthquakes, we assume that the residual part of the long-term trend (a few tenths of millimeter per year since ca. 1895) is related to interseismic loading at the century scale. Though we need a more precise measurement of the regional sea level rise and more data along the Lesser Antilles arc to better constrain the rates of vertical deformation and its source, a simple elastic dislocation model allows us to discuss the behavior of the megathrust at the century scale. We found that 1 mm/yr of subsidence on the Caravelle peninsula could be explained by interseismic loading on an interface fully locked down to 60 km depth. This would be in disagreement with *Manaker et al.* [2008] and *Symithe et al.* [2015], who estimated low coupling offshore Martinique by using GPS. However, it is questionable whether the coupling estimated from a short and sparse geodetic record is representative of the long-term megathrust behavior.

Similarities between the deep behavior of the NE Japan megathrust and the Lesser Antilles megathrust, previously noted by *Laigle et al.* [2013] and *Satriano et al.* [2014], seem to be confirmed by our study. Indeed, both the *M*7+ 1946 earthquake and the *M*8 1839 historical earthquake likely nucleated in the mantle wedge, and to explain the long-term submergence recorded by microatolls, deep interseismic loading on a locked segment below the forearc Moho is needed. Overall, our results imply that the seismogenic interface likely does not stop at the crust-mantle boundary but extends below the forearc Moho, as already suggested by *Ruiz et al.* [2013] and *Laigle et al.* [2013]. Such a downward extension of the seismogenic interface into the mantle wedge was also observed in Sumatra [*Simoes et al.*, 2004; *Singh et al.*, 2008; *Dessa et al.*, 2009]. Likewise, the downdip limit of the seismogenic segment of the NE Japan subduction zone is below the forearc Moho [*Seno*, 2005; *Suwa et al.*, 2006; *Igarashi et al.*, 2001]. Indeed, numerous repeating earthquakes of magnitude 7–8 occurred at depth below the forearc Moho and the large 2011 Tohoku rupture reached the slab-mantle interface [e.g., *Satriano et al.*, 2014]. *Laigle et al.* [2013] previously discussed similarities between the deep seismic behavior of the Lesser Antilles megathrust and that in NE Japan. The lack of tremors and slow earthquakes and the sustained seismic activity in the mantle corner for both the Tohoku and the Lesser Antilles subduction zones have suggested that the mantle wedge in both cases has a different composition than classic lithospheric mantle [*Laigle et al.*, 2013]. A heterogenous mantle with pyroxenite has been proposed to enable stick-slip behavior on some part of the slab-forearc mantle contact and allow the downward extension of the seismogenic segment [*Laigle et al.*, 2013]. This particular chemical composition of the lithospheric forearc mantle would be related to its history of formation and evolution [*Laigle et al.*, 2013]. The resemblance between these two subduction zones could be used as a key to better characterization of the long-term seismic activity of the Lesser Antilles megathrust [*Laigle et al.*, 2013; *Satriano et al.*, 2014]. For example, as it occurred during the 2011 Tohoku event [e.g., *Ozawa et al.*, 2012], the deep seismic activity of the Lesser Antilles megathrust, with moderate earthquakes, could load the shallower segment and instigate a larger megathrust earthquake.

Appendix A: U/Th Dating for Microatolls

U-Th analysis of the two Raisin 1 and Raisin 2 microatolls were carried out by Thermo-Ionization Mass Spectrometry (VG-54) at CEREGE, Aix-en-Provence, following the procedure described in *Deschamps et al.* [2012]. Prior to U-Th analyses, X-ray diffraction analyses were performed on both samples and indicated no post-mortem diagenetic alteration of their aragonite skeletons. The typical precision of the [^{230}Th/^{238}U] ratio on very young samples (less than a few decades old) is about 2–3%, leading to an uncertainty of a few years for a sample age of 50 years. Because these samples are very young, U-Th age calculations require correction for the nonradiogenic ^{230}Th fraction. Similarly to the approach proposed by *Cobb et al.* [2003], the ^{230}Th/^{232}Th signature of the nonradiogenic thorium was estimated by comparing measured U-Th ages to absolute dates for coral of a known age. Such an approach leads to an initial ^{230}Th/^{232}Th activity ratio of 1.30 ± 0.65 for Raisin 1 samples and 2.6 ± 1.3 for Raisin 2 samples. Note that a systematic uncertainty of 50% is assumed on these estimates and propagated to the final corrected U-Th ages. Ultimately, the absolute U-Th ages obtained for the three samples are 1781.6 ± 6.4 (Raisin 1-1), 1908.0 ± 7.2 (Raisin 1-2), and 1886.6 ± 5.2 (Raisin 2) (see Table 1).

Appendix B: Computing Method for Estimating Uncertainties in Growth Band Counting

To estimate the uncertainty of our growth band counting, we have developed a computing tool. The method is based on a semi-automatic counting of growth bands along a profile that we selected on the X-ray image. The whole profile is divided in several smaller overlapping profiles, which enables the estimation of the evolution of the uncertainty through time (with an increasing number of counted bands). After numerous tests, we have concluded that it is most important to select the clearest profile on which to apply the calculation. Finally, because each X-ray is different (in terms of resolution and readability), automatic countings were done independently.

The method consists of the selection of one initial profile, manually outlined in the X-ray image, for which the program calculates a gray level curve (Figures S1a and S1b). This raw curve is composed of numerous oscillations including the annual signal of the coral growth we are targeting (Figure S1b). In order to isolate this particular signal, we use a second-order bandpass Butterworth filter. Adjusting the range of frequencies allows us to choose the peaks that we identify as corresponding to the annual signal (Figure S1b). Once the filter is adjusted, we obtain a filtered signal in which the peaks are automatically counted (Figure S1b). By repeating the calculation 200 times on profiles shifted by ± 20 pixels compared to the initial profile, we obtain a Gaussian-shaped histogram. From this distribution (Figure S1c), we infer the median value of the number of counted bands and the corresponding 2σ uncertainty. The goal of the random profiles is to laterally average the number of counted bands to represent the typical variability of readability of the X-ray. The median values obtained with this method are very similar to the full manual counting results.

For each X-ray on which we applied the computing method, we inferred a linear relation between the number of counted bands and the counting uncertainty. An example is given in Figure S2a. By considering all X-rays (12 X-rays from corals sampled in the Antilles), we estimated that on average, the 2σ uncertainties are around ± 2 years, ± 3.5 years, ± 5 years, and ± 6 years for annual bands that are 50, 100, 150, and 200 years old, respectively (Figure S2b). For the most easily readable X-rays, uncertainty increases more slowly, with an uncertainty of ± 4 years for a 200 years old sample for Ecurie 4 and SFRZ2-1, while for other X-rays, the uncertainty can reach ± 10 years for a 200 years old sample (Figure S2b).

Acknowledgments

We thank Frédérique Leclerc, Yann Klinger, and Bruno Hamelin for helpful discussions. A special thanks to Belle Philibosian for the fruitful proofreadings and very helpful discussions. We sincerely thank Benoît Taisne of the Earth Observatory of Singapore, who helped us to model the volcanoes' impact on the relative sea level changes. Thanks to Guy Wöppelmann of the LIttoral ENvironnement et Sociétés (LIENSs) for his help in improving our discussion of the regional sea level rise with the use of GPS records. The fieldwork required help from the Volcanologic and Seismologic Observatory of Martinique, and we sincerely thank the whole observatory team for their logistic help and their participation in the field. We thank Christophe Yvon for underwater photography. Thanks to the Saint-Paul clinic of Fort-de-France for the free X-rays of coral slices and for their interest in the research project. Thanks to Cyril Giry for help in estimating counting uncertainties. Pierre Deschamps is supported by the Agence Nationale de la Recherche (Project EQUIPEX ASTER-CEREGE). The project was funded by the ANR CATTELL SUBSISMANTI and the INSU (CT3 ALEAS). Data are included in the main text and supporting information files as figures; any additional information may be obtained on request at IPGP email: weilaccardo@ipgp.fr. This is IPGP contribution 3727.

References

Beauducel, F., S. Bazin, M. Bengoubou-Valerius, M.-P. Bouin, A. Bosson, C. Anténor-Habazac, V. Clouard, and J.-B. De Chabalier (2011), Empirical model for rapid macroseismic intensities prediction in Guadeloupe and Martinique, *C. R. Geosci.*, *343*(11), 717–728.

Blum, M. D., and H. H. Roberts (2009), Drowning of the Mississippi Delta due to insufficient sediment supply and global sea-level rise, *Nat. Geosci.*, *2*(7), 488–491.

Boudon, G. (2011), Les volcans actifs de l'outre-mer français, des édifices à haut risque, *Geosciences*, *14*, 76–83.

Bouin, M., and G. Wöppelmann (2010), Land motion estimates from GPS at tide gauges: A geophysical evaluation, *Geophys. J. Int.*, *180*(1), 193–209.

Bowin, C. (1976), *Caribbean Gravity Field and Plate Tectonics*, pp. 168–170, Geol. Soc. Am., Boulder, Colo.

Briggs, R. W., et al. (2006), Deformation and slip along the Sunda megathrust in the great 2005 Nias-Simeulue earthquake, *Science*, *311*(5769), 1897–1901.

Chlieh, M., J. De Chabalier, J. Ruegg, R. Armijo, R. Dmowska, J. Campos, and K. Feigl (2004), Crustal deformation and fault slip during the seismic cycle in the North Chile subduction zone, from GPS and InSAR observations, *Geophys. J. Int.*, *158*(2), 695–711.

Clark, J. A., W. E. Farrell, and W. R. Peltier (1978), Global changes in postglacial sea level: A numerical calculation, *Quat. Res.*, *9*(3), 265–287.

Cobb, K. M., C. D. Charles, H. Cheng, M. Kastner, and R. L. Edwards (2003), U/Th-dating living and young fossil corals from the central tropical Pacific, *Earth Planet. Sci. Lett.*, *210*(1), 91–103.

DeMets, C., P. E. Jansma, G. S. Mattioli, T. H. Dixon, F. Farina, R. Bilham, E. Calais, and P. Mann (2000), GPS geodetic constraints on Caribbean-North America plate motion, *Geophys. Res. Lett.*, *27*(3), 437–440.

Deschamps, P., N. Durand, E. Bard, B. Hamelin, G. Camoin, A. L. Thomas, G. M. Henderson, J. Okuno, and Y. Yokoyama (2012), Ice-sheet collapse and sea-level rise at the Bolling warming 14,600 years ago, *Nature*, *483*(7391), 559–564.

Dessa, J.-X., et al. (2009), Megathrust earthquakes can nucleate in the forearc mantle: Evidence from the 2004 Sumatra event, *Geology*, *37*(7), 659–662.

Dorel, J. (1981), Seismicity and seismic gap in the Lesser Antilles arc and earthquake hazard in Guadeloupe, *Geophys. J. Int.*, *67*(3), 679–695.

Douglas, B. C., and W. R. Peltier (2002), The puzzle of global sea-level rise, *Phys. Today*, *55*(3), 35–41.

Evain, M., A. Galve, P. Charvis, M. Laigle, H. Kopp, A. Bécel, W. Weinzierl, A. Hirn, E. R. Flueh, and J. Gallart (2013), Structure of the Lesser Antilles subduction forearc and backstop from 3D seismic refraction tomography, *Tectonophysics*, *603*, 55–67.

Feuillard, M. (1985), Macrosismicit de la Guadeloupe et de la Martinique, Observatoire volcanologique de la SoufriŔre (Guadeloupe).

Feuillet, N. (2000), Sismotectonique des petites antilles liaison entre activit sismique et volcanique, PhD thesis, Institut de Physique du Globe de Paris.

Feuillet, N., I. Manighetti, P. Tapponnier, and E. Jacques (2002), Arc parallel extension and localization of volcanic complexes in Guadeloupe, Lesser Antilles, *J. Geophys. Res.*, *107*(B12), 2331, doi:10.1029/2001JB000308.

Feuillet, N., P. Tapponnier, I. Manighetti, B. Villemant, and G. King (2004), Differential uplift and tilt of Pleistocene reef platforms and Quaternary slip rate on the Morne-Piton normal fault (Guadeloupe, French West Indies), *J. Geophys. Res.*, *109*, B02404, doi:10.1029/2003JB002496.

Feuillet, N., F. Beauducel, and P. Tapponnier (2011a), Tectonic context of moderate to large historical earthquakes in the Lesser Antilles and mechanical coupling with volcanoes, *J. Geophys. Res.*, *116*, B10308, doi:10.1029/2011JB008443.

Feuillet, N., F. Beauducel, E. Jacques, P. Tapponnier, B. Delouis, S. Bazin, M. Vallée, and G. King (2011b), The Mw = 6.3, November 21, 2004, Les Saintes earthquake (Guadeloupe): Tectonic setting, slip model and static stress changes, *J. Geophys. Res.*, *116*, B10301, doi:10.1029/2011JB008310.

Garnier, E., J. Desarthe, and D. Moncoulon (2015), The historic reality of the cyclonic variability in French Antilles, 1635–2007, *Clim. Past Discuss.*, *11*(2), 1519–1550.

Gutenberg, B., and C. F. Richter (1954), *Seismicity of the Earth and Related Phenomena*, Princeton Univ. Press, Princeton, N. J.

Holgate, S. J., A. Matthews, P. L. Woodworth, L. J. Rickards, M. E. Tamisiea, E. Bradshaw, P. R. Foden, K. M. Gordon, S. Jevrejeva, and J. Pugh (2012), New data systems and products at the permanent service for mean sea level, *J. Coastal Res.*, *29*(3), 493–504.

Hopley, D. (2011), *Encyclopedia of Modern Coral Reefs: Structure, Form and Process*, Springer, Netherlands.

Igarashi, T., T. Matsuzawa, N. Umino, and A. Hasegawa (2001), Spatial distribution of focal mechanisms for interplate and intraplate earthquakes associated with the subducting Pacific plate beneath the northeastern Japan arc: A triple-planed deep seismic zone, *J. Geophys. Res.*, *106*(B2), 2177–2191.

Kanamori, H. (1977), The energy release in great earthquakes, *J. Geophys. Res.*, *82*(20), 2981–2987.

Kanda, R. V., and M. Simons (2010), An elastic plate model for interseismic deformation in subduction zones, *J. Geophys. Res.*, *115*, B03405, doi:10.1029/2009JB006611.

Kemp, A. C., B. P. Horton, S. J. Culver, D. R. Corbett, O. van de Plassche, W. R. Gehrels, B. C. Douglas, and A. C. Parnell (2009), Timing and magnitude of recent accelerated sea-level rise (North Carolina, United States), *Geology*, *37*(11), 1035–1038.

Kemp, A. C., B. P. Horton, J. P. Donnelly, M. E. Mann, M. Vermeer, and S. Rahmstorf (2011), Climate related sea-level variations over the past two millennia, *Proc. Natl. Acad. Sci. U.S.A.*, *108*(27), 11,017–11,022.

Laigle, M., et al. (2013), Seismic structure and activity of the north-central Lesser Antilles subduction zone from an integrated approach: Similarities with the Tohoku forearc, *Tectonophysics*, *603*, 1–20.

Leclerc, F. (2014), Déformation active permanente induite par le méga-chevauchement dans l'arc antillais: Apport des complexes récifaux quaternaires, PhD thesis, Institut de Physique du Globe de Paris.

Leclerc, F., N. Feuillet, M. Perret, G. Cabioch, S. Bazin, J.-F. Lebrun, and J. Saurel (2015), The reef platform of Martinique: Interplay between eustasy, tectonic subsidence and volcanism since Late Pleistocene, *Mar. Geol.*, *369*, 34–51.

Manaker, D. M., E. Calais, A. Freed, S. Ali, P. Przybylski, G. Mattioli, P. Jansma, C. Prépetit, and J. De Chabalier (2008), Interseismic plate coupling and strain partitioning in the northeastern Caribbean, *Geophys. J. Int.*, *174*(3), 889–903.

Meteorological Service of the Netherlands Antilles and Aruba (2010), Hurricanes and tropical storms in the Netherlands Antilles and Aruba, *Tech. Rep.*, Meteorol. Serv. Netherlands Antilles and Aruba.

Meltzner, A. J. (2010), Earthquake recurrence, clustering and persistent segmentation near the southern end of the 2004 Sunda megathrust rupture, PhD thesis, Pasadena, Calif.

Meltzner, A. J., K. Sieh, M. Abrams, D. C. Agnew, K. W. Hudnut, J.-P. Avouac, and D. H. Natawidjaja (2006), Uplift and subsidence associated with the great Aceh-Andaman earthquake of 2004, *J. Geophys. Res.*, *111*, B02407, doi:10.1029/2005JB003891.

Meltzner, A. J., K. Sieh, H.-W. Chiang, C.-C. Shen, B. W. Suwargadi, D. H. Natawidjaja, B. E. Philibosian, R. W. Briggs, and J. Galetzka (2010), Coral evidence for earthquake recurrence and an AD 1390–1455 cluster at the south end of the 2004 Aceh–Andaman rupture, *J. Geophys. Res.*, *115*, B10402, doi:10.1029/2010JB007499.

Meltzner, A. J., K. Sieh, H.-W. Chiang, C.-C. Shen, B. W. Suwargadi, D. H. Natawidjaja, B. Philibosian, and R. W. Briggs (2012), Persistent termini of 2004- and 2005-like ruptures of the Sunda megathrust, *J. Geophys. Res.*, *117*, B04405, doi:10.1029/2011JB008888.

Meltzner, A. J., et al. (2015), Time-varying interseismic strain rates and similar seismic ruptures on the Nias-Simeulue patch of the Sunda megathrust, *Quat. Sci. Rev.*, *122*, 258–281.

Meyssignac, B., D. Salas y Melia, M. Becker, W. Llovel, and A. Cazenave (2012), Tropical Pacific spatial trend patterns in observed sea level: Internal variability and/or anthropogenic signature?, *Clim. Past*, *8*(2), 787–802.

Mogi, K. (1958), Relations between the eruptions of various volcanoes and the deformations of the ground surfaces around them, *Bull. Earthquake Res. Inst.*, *36*, 99–134.

Natawidjaja, D. H., K. Sieh, S. N. Ward, H. Cheng, R. L. Edwards, J. Galetzka, and B. W. Suwargadi (2004), Paleogeodetic records of seismic and aseismic subduction from central Sumatran microatolls, Indonesia, *J. Geophys. Res.*, *109*, B04306, doi:10.1029/2003JB002398.

Natawidjaja, D. H., K. Sieh, M. Chlieh, J. Galetzka, B. W. Suwargadi, H. Cheng, R. L. Edwards, J.-P. Avouac, and S. N. Ward (2006), Source parameters of the great Sumatran megathrust earthquakes of 1797 and 1833 inferred from coral microatolls, *J. Geophys. Res.*, *111*, B06403, doi:10.1029/2005JB004025.

Natawidjaja, D. H., K. Sieh, J. Galetzka, B. W. Suwargadi, H. Cheng, R. L. Edwards, and M. Chlieh (2007), Interseismic deformation above the Sunda megathrust recorded in coral microatolls of the Mentawai islands, West Sumatra, *J. Geophys. Res.*, *112*, B02404, doi:10.1029/2006JB004450.

Newman, A. V., et al. (2012), Recent geodetic unrest at Santorini Caldera, Greece, *Geophys. Res. Lett.*, *39*, L06309, doi:10.1029/2012GL051286.

Okada, Y. (1992), Internal deformation due to shear and tensile faults in a half-space, *Bull. Seismol. Soc. Am.*, *82*(2), 1018–1040.

Ozawa, S., T. Nishimura, H. Munekane, H. Suito, T. Kobayashi, M. Tobita, and T. Imakiire (2012), Preceding, coseismic, and postseismic slips of the 2011 Tohoku earthquake, Japan, *J. Geophys. Res.*, *117*, B07404, doi:10.1029/2011JB009120.

Palanisamy, H., M. Becker, B. Meyssignac, O. Henry, and A. Cazenave (2012), Regional sea level change and variability in the Caribbean sea since 1950, *J. Geod. Sci.*, *2*(2), 125–133.

Penland, S., and K. E. Ramsey (1990), Relative sea-level rise in Louisiana and the Gulf of Mexico: 1908–1988, *J. Coastal Res.*, *6*, 323–342.

Philibosian, B., K. Sieh, D. H. Natawidjaja, H.-W. Chiang, C.-C. Shen, B. W. Suwargadi, E. M. Hill, and R. L. Edwards (2012), An ancient shallow slip event on the Mentawai segment of the Sunda megathrust, Sumatra, *J. Geophys. Res.*, *117*, B05401, doi:10.1029/2011JB009075.

Philibosian, B., K. Sieh, J.-P. Avouac, D. H. Natawidjaja, H.-W. Chiang, C.-C. Wu, H. Perfettini, C.-C. Shen, M. R. Daryono, and B. W. Suwargadi (2014), Rupture and variable coupling behavior of the Mentawai segment of the Sunda megathrust during the supercycle culmination of 1797 to 1833, *J. Geophys. Res. Solid Earth*, *119*, 7258–7287, doi:10.1002/012014JB011200.

Robson, G. (1964), An earthquake catalogue for the Eastern Caribbean 1530–1960, *Bull. Seismol. Soc. Am.*, *54*(2), 785–832.

Ruiz, M., et al. (2013), Seismic activity offshore Martinique and Dominica islands (Central Lesser Antilles subduction zone) from temporary onshore and offshore seismic networks, *Tectonophysics*, *603*, 68–78.

Russo, R. M., E. A. Okal, and K. C. Rowley (1992), Historical seismicity of the southeastern Caribbean and tectonic implications, *Pure Appl. Geophys.*, *139*(1), 87–120.
Satriano, C., V. Dionicio, H. Miyake, N. Uchida, J.-P. Vilotte, and P. Bernard (2014), Structural and thermal control of seismic activity and megathrust rupture dynamics in subduction zones: Lessons from the Mw 9.0, 2011 Tohoku earthquake, *Earth Planet. Sci. Lett.*, *403*, 287–298.
Savage, J. (1983), A dislocation model of strain accumulation and release at a subduction zone, *J. Geophys. Res.*, *88*(B6), 4984–4996.
Savry, C. (2007), Etude morpho-tectonique de la Martinique, partie nord-ouest, Master's thesis, Université Blaise Pascal et Institut de Physique du Globe de Paris.
Scoffin, T. P., D. Stoddart, and B. R. Rosen (1978), The nature and significance of microatolls, *Philos. Trans. R. Soc. B*, *284*(999), 99–122.
Seno, T. (2005), Variation of downdip limit of the seismogenic zone near the Japanese islands: Implications for the serpentinization mechanism of the forearc mantle wedge, *Earth Planet. Sci. Lett.*, *231*(3), 249–262.
Sieh, K., D. H. Natawidjaja, A. J. Meltzner, C.-C. Shen, H. Cheng, K.-S. Li, B. W. Suwargadi, J. Galetzka, B. Philibosian, and R. L. Edwards (2008), Earthquake supercycles inferred from sea-level changes recorded in the corals of west Sumatra, *Science*, *322*(5908), 1674–1678.
Simoes, M., J. P. Avouac, R. Cattin, and P. Henry (2004), The Sumatra subduction zone: A case for a locked fault zone extending into the mantle, *J. Geophys. Res.*, *109*, B10402, doi:10.1029/2003JB002958.
Singh, S. C., et al. (2008), Seismic evidence for broken oceanic crust in the 2004 Sumatra earthquake epicentral region, *Nat. Geosci.*, *1*(11), 777–781.
Smithers, S. G., and C. D. Woodroffe (2001), Coral microatolls and 20th century sea level in the eastern Indian Ocean, *Earth Planet. Sci. Lett.*, *191*(1), 173–184.
Sparks, R. S. J., et al. (1998), Magma production and growth of the lava dome of the Soufriere Hills Volcano, Montserrat, West Indies: November 1995 to December 1997, *Geophys. Res. Lett.*, *25*(18), 3421–3424.
Stoddart, D. R., and T. P. Scoffin (1979), *Microatolls: Review of Form, Origin, and Terminology, Atoll Res. Bull*, *224*, 17 pp.
Suwa, Y., S. Miura, A. Hasegawa, T. Sato, and K. Tachibana (2006), Interplate coupling beneath NE Japan inferred from three-dimensional displacement field, *J. Geophys. Res.*, *111*, B04402, doi:10.1029/2004JB003403.
Symithe, S., E. Calais, J. Chabalier, R. Robertson, and M. Higgins (2015), Current block motions and strain accumulation on active faults in the Caribbean, *J. Geophys. Res. Solid Earth*, *120*, 3748–3774, doi:10.1002/2014JB011779.
Tamisiea, M. E., and J. X. Mitrovica (2011), The moving boundaries of sea level change: Understanding the origins of geographic variability, *Oceanography*, *24*(2), 24–39, doi:10.5670/oceanog.2011.25.
Taylor, F., B. Isacks, C. Jouannic, A. Bloom, and J. Dubois (1980), Coseismic and Quaternary vertical tectonic movements, Santo and Malekula Islands, New Hebrides island arc, *J. Geophys. Res.*, *85*(B10), 5367–5381.
Taylor, F. W., C. Jouannic, L. Gilpin, and A. Bloom (1982), Coral colonies as monitors of change in relative level of the land and sea: Applications to vertical tectonism, paper presented at 4th Int. Coral Reef Congress, Manila, 5 May.
Taylor, F. W., C. Frohlich, J. Lecolle, and M. Strecker (1987), Analysis of partially emerged corals and reef terraces in the central Vanuatu arc: Comparison of contemporary coseismic and nonseismic with Quaternary vertical movements, *J. Geophys. Res.*, *92*(B6), 4905–4933.
Torres, R. R., and M. N. Tsimplis (2013), Sea-level trends and interannual variability in the Caribbean Sea, *J. Geophys. Res. Oceans*, *118*, 2934–2947, doi:10.1002/jgrc.20229.
Weil-Accardo, J. (2014), Variations séculaires du niveau marin relatif liées au fonctionnement du méga-chevauchement et au climat dans les Antilles: Apport des microatolls coralliens, PhD thesis, Institut de Physique du Globe de Paris.
Weil-Accardo, J., N. Feuillet, E. Jacques, P. Deschamps, J.-M. Saurel, K. Thirumalai, S. Demeza, and D. Anglade (2016), Relative sea-level changes during the last century recorded by coral microatolls in Belloc, Haiti, *Global Planet. Change*, *139*, 1–14, doi:10.1016/j.gloplacha.2015.12.019.
Wells, D. L., and K. J. Coppersmith (1994), New empirical relationships among magnitude, rupture length, rupture width, rupture area, and surface displacement, *Bull. Seismol. Soc. Am.*, *84*(4), 974–1002.
Westbrook, G., J. Ladd, P. Buhl, N. Bangs, and G. Tiley (1988), Cross section of an accretionary wedge: Barbados Ridge complex, *Geology*, *16*(7), 631–635.
Woodroffe, C., and R. McLean (1990), Microatolls and recent sea level change on coral atolls, *Nature*, *344*, 531–534.
Woodroffe, C., R. McLean, H. Polach, and E. Wallensky (1990), Sea level and coral atolls: Late Holocene emergence in the Indian Ocean, *Geology*, *18*(1), 62–66.
Woodroffe, C. D., and M. K. Gagan (2000), Coral microatolls from the central Pacific record late Holocene El Niño, *Geophys. Res. Lett.*, *27*(10), 1511–1514.
Woodroffe, C. D., H. V. McGregor, K. Lambeck, S. G. Smithers, and D. Fink (2012), Mid-Pacific microatolls record sea-level stability over the past 5000 yr, *Geology*, *40*(10), 951–954.
Wöppelman, G., and M. Marcos (2015), Le paradoxe de lèlévation du niveau des mers au xxe siŔcle, *Revue XYZ*, *143*, 29–36.
Wöppelmann, G., C. Letetrel, A. Santamaria, M.-N. Bouin, X. Collilieux, Z. Altamimi, S. Williams, and B. M. Miguez (2009), Rates of sea-level change over the past century in a geocentric reference frame, *Geophys. Res. Lett.*, *36*, L12607, doi:10.1029/2009GL038720.
Young, S. R., R. S. J. Sparks, W. P. Aspinall, L. L. Lynch, A. D. Miller, R. E. Robertson, and J. B. Shepherd (1998), Overview of the eruption of Soufriere Hills volcano, Montserrat, 18 July 1995 to December 1997, *Geophys. Res. Lett.*, *25*(18), 3389–3392.
Yu, K.-F., J.-X. Zhao, T. Done, and T.-G. Chen (2009), Microatoll record for large century-scale sea-level fluctuations in the mid-Holocene, *Quat. Res.*, *71*(3), 354–360.
Zachariasen, J., K. Sieh, F. W. Taylor, R. L. Edwards, and W. S. Hantoro (1999), Submergence and uplift associated with the giant 1833 Sumatran subduction earthquake: Evidence from coral microatolls, *J. Geophys. Res.*, *104*(B1), 895–919.
Zachariasen, J., K. Sieh, F. W. Taylor, and W. S. Hantoro (2000), Modern vertical deformation above the Sumatran subduction zone: Paleogeodetic insights from coral microatolls, *Bull. Seismol. Soc. Am.*, *90*(4), 897–913.
Zachariasen, J. A. (1998), Paleoseismology and paleogeodesy of the Sumatran subduction zone: A study of vertical deformation using coral microatolls, PhD thesis, Calif. Inst. of Tech., Pasadena, Calif.
Zahibo, N., I. Nikolkina, and I. Didenkulova (2008), Extreme waves generated by cyclones in Guadeloupe, in *Extreme Ocean Waves*, edited by E. Pelinovsky and C. Kharif, pp. 159–177, Springer, Netherlands.